Development of Structures and Methods for Safe On Orbit Robotic Assembly of Small Satellites

by

Mary Dahl

S.B., Massachusetts Institute of Technology (2020)

Submitted to the Department of Aeronautics and Astronautics
in partial fulfillment of the requirements for the degree of

Master of Science in Aeronautics and Astronautics

at the

MASSACHUSETTS INSTITUTE OF TECHNOLOGY

May 2022

Author . . . .
Department of Aeronautics and Astronautics
May 17, 2022

Certified by. . . . .
Kerri Cahoy
Associate Professor and Bisplinghoff Faculty Fellow
Thesis Supervisor

Accepted by . . . .
Jonathan P. How
R. C. Maclaurin Professor of Aeronautics and Astronautics
Chair, Graduate Program Committee

This page is intentionally blank.

Development of Structures and Methods for Safe On Orbit Robotic Assembly of Small Satellites

by

Mary Dahl

Submitted to the Department of Aeronautics and Astronautics
on May 17, 2022, in partial fulfillment of the
requirements for the degree of
Master of Science in Aeronautics and Astronautics

Abstract

While the advent of small satellites such as CubeSats have allowed for space to become quicker and easier to access, the turn-around time is still insufficient for rapid deployment. Example situations are replacing nodes in large constellations, time-sensitive science experiments, or disaster relief imaging. A solution can be found in on-orbit assembly. By flat packing a large quantity of snap-fit compatible boards for a plurality of CubeSats and assembling them on-orbit, time from conception to operation can be significantly lowered. Crucial to on-orbit robotic assembly is the design of the satellite. Traditional CubeSats, with rails, precise pin connectors, dense headers, and small wires, are difficult to assemble for all but the most advanced robots. Instead, this thesis discusses the design and testing of custom-made structures for assembly by a Cartesian robot with an electromagnetic end effector. These structural designs need to ensure consistent, repeatable, and safe assembly of satellites, both on the ground and on orbit. The requirements for such a system are examined with a Systems Theoretic Process Analysis, or STPA. Additionally, different types of compliant design features, such as sliding latches and chamfer overhangs, have their performance analyzed by performing repeated insertion tests. It is found that, with compliant designs, a Cartesian robot can assemble the designed structure of eight boards and four rails in approximately four minutes.

Thesis Supervisor: Kerri Cahoy
Title: Associate Professor and Bisplinghoff Faculty Fellow

This page is intentionally blank.

Acknowledgments

This thesis wasn't solely created by me; it was fueled by the support I received from all the people around me who believed in me. I started grad school in a flurry of motion during a global pandemic, following a project I firmly believed in but couldn't touch. Through trial, error, starts, and restarts, I've finally been able to produce something that means something, and will hopefully be the first step to me making space a more sustainable place in the future. I would like to take this time to thank everyone who made this at all possible.

Thank you, first and foremost, to my family at home. We weathered a lot these past few years, and it's difficult to really express how much you have meant to me all my life. Even now that I've moved away (and you may or may not have replaced me with a beautiful cat I haven't even met yet), I think of you all every day and am eternally grateful for all the love and support I was given growing up.

To my roommates and best friends in the entire world, Jeremy, Jamie, and Kendall. This past year has been just as wonderful as I'd always hoped. From cooking to D&D nights to video games to letting me talk your ears off about whatever thing has caught my interest lately, thank you, thank you, for everything.

To the entire Matrix team – Ezinne, Meng, Emily, Shreya, Pablo, Codrin, Maggie, Izzie, and anyone who has lent an ear or a suggestion – some of you have come and gone, but your contributions were indispensable, no matter how small you may have thought they were. Thank you for helping to bring this wild project into the world, especially during a pandemic.

Thank you to Rob and everyone at Momentus for funding Matrix and for the invaluable advice and feedback.

And, of course, above all else, thank you to Kerri Cahoy, the best advisor anyone could ask for. Your dedication to each and every one of your students is unfathomable. You have helped me in ways beyond this thesis, and I'm looking forward to continuing to work with you moving forward.

This page is intentionally blank.

Contents

This page is intentionally blank.

List of Figures

List of Tables

This page is intentionally blank.

Chapter 1

Introduction

1.1 Motivation for On-Orbit Assembly

The accessibility of space has increased greatly in recent years with the advent of CubeSat ridesharing programs, allowing more satellites than ever to get into orbit. Yearly launches have been as many as 297 in 2017, and hundreds more have been announced for upcoming years [18]. With this ease of access also comes the possibility for individual organizations to launch greater numbers of satellites in inter-working constellations, such as those by Planet and SpaceX. Constellations greatly increase the amount of work that can be done in the lifespan of a low Earth orbit satellite, both by spatially having increased ground coverage for Earth observation or other services, as well as being able to utilize cross-link communications to optimize the quantity of data returned to the ground. Storms could be better monitored, air traffic control could be improved, and internet could be provided to remote locations; all available with more ease and speed than ever before. CubeSats are the next step in an ever-evolving industry of smaller, faster, and better satellites, but this rapid-but-not-instant turnover offers several problems.

CubeSats are not highly reliable. Although learned best practices and flight heritage have increased the rate of CubeSat success from their introduction, many still fail; as of 2018, 21% of CubeSats suffered on-orbit failure, and 12% had launch failures [37]. These failures range in source, from antennas not deploying, to malfunctioning

boards, to radiation to on-orbit conjunctions. As launches move to hundreds or thousands of co-working small satellites, this problem is only exacerbated, as many constellation missions rely on most nodes being functional for full efficiency of mission. When a node fails, in the best scenario, the constellation has limited functionality, with increased data latency and/or decreased data volume. In the worst case, the mission ends. Replacement of broken nodes takes months of testing and approval, even if that exact CubeSat design has already been launched, and waiting for a launch opportunity that coincides with the desired orbit. The current "solution" to this problem is simply to launch more satellites in the initial release, as this redundancy can help the mission continue even if individual nodes go down.

Launching replacement satellites is infeasible for several reasons. First and foremost: cost. Smaller constellations of less than ten satellites often cannot afford to send up redundant nodes, both for the cost of the satellite itself and for the launch opportunity. Without owning a fleet of rockets, launching more than one satellite, and to that point, hundreds or thousands, to achieve the desired robustness to satellite failure is incredibly costly. Companies such as Iridium and OneWeb have entered bankruptcy trying to deploy their proposed constellations.

Even if money is not an issue, giant constellations for the sake of redundancies bring dangers to the sustainability of Earth orbit. Taking Starlink as an example: as of November 2020 Starlink has launched 895 satellites and experienced approximately 2.5% failure [20], or approximately 22 satellites. This amount is not a crisis on its own, but as Starlink plans to continue to expand to over 40,000 satellites, and at that level of failure, 1,000 satellites can cause conjunctions, orbital debris, and a congested orbit.

All these factors combined creates the need to get satellites of a known design to their required orbit faster, such that constellations can be smaller and more efficient. An opportunity arises in on-orbit manufacturing and assembly. By building CubeSats on-orbit, the time consuming test and launch steps can be skipped entirely, allowing for a faster concept to space timeline. It also means that the satellites don't need to be designed to survive the launch environment, which allows them to be less
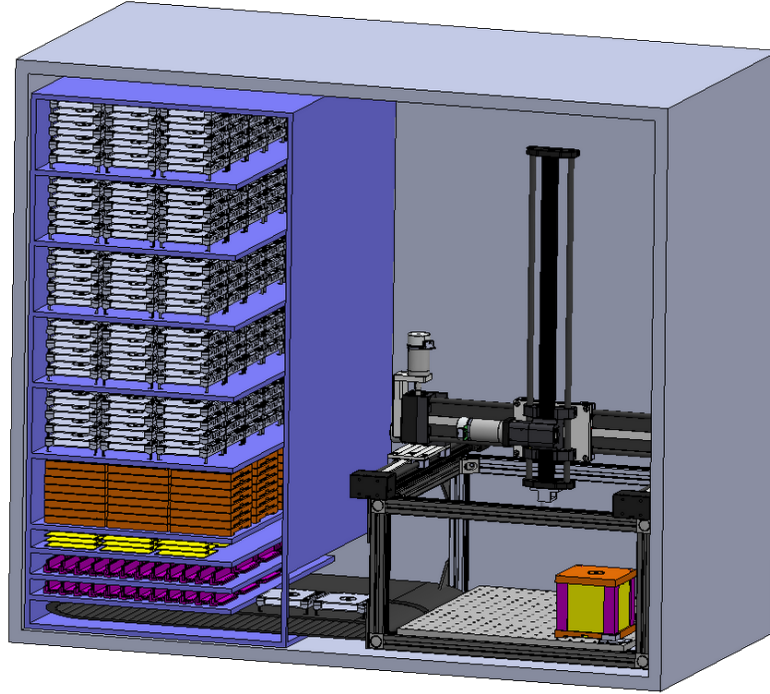
Figure 1-1: A model of the proposed locker. A Cartesian robot assembles parts into CubeSats, after which they are ejected into orbit (not shown). The parts are flat-packed to allow for maximum volume of CubeSats able to be constructed. They are delivered to the assembly area via a secondary robot grabber (not shown) and a timing belt. (Mary Dahl, MIT, Rev 2, January 2022)

robust and more lightweight, opening up the design space for structures and payloads. Constellations could be fully assembled and deployed directly into their orbital slots by the construction unit, reducing the need for propulsion systems on the satellites themselves. If a node in a constellation goes down, the on-orbit "factory" could construct and deploy a replacement node.

A potential version of this system could be an orbital robotic assembly system. A "locker" of modular CubeSat parts would be stored and, on command, a robot would assemble them into CubeSats of different configurations. A concept sketch of this system can be seen in Figure 1-1. This CubeSat locker could be located in several different orbits and self-propel as necessary to deliver CubeSats into any orbit, all without needing another rocket launch.

A locker like this naturally brings to mind a simpler solution of storing pre-made constellation nodes on orbit and deploying them as necessary as replacement nodes.

There are several benefits to the flexibility a robotic construction system provides. First, flat packing satellite parts allows for more total satellites to be deployed, even taking into account the volume the robot takes up [34]. It also allows for the locker to perform a secondary mission of assembling simple CubeSats on command. All boards on the locker would be compatible with each other, so, utilizing a simple payload such as a camera or an AI board, a custom CubeSat could be constructed for an on-demand satellite missions. This could be utilized for any number of purposes, such as rapid imaging responses to natural disasters or for performing technology tests for educational purposes.

To perform on-orbit satellite construction, four key areas must be explored: robot programming, modular structure design, locker system design, and operation schedule and optimization. Previous and ongoing work is examining different aspects of programming, structural designs, and operations [34] [35] [36], but an in-depth analysis of a modular structure design is still necessary. A 3D printed, custom CubeSat structure that can be assembled in different configurations for different types of missions would provide the flexibility for balancing both goals of replacing constellation nodes and rapid, simple satellite deployment for this work.

1.2 Background

There has been much work in the fields of both on-orbit manufacturing and in innovative, 3D printed CubeSat structures. Combining these two fields is the crux of the work in this thesis. A structure that is designed at the same time as the robot system offers several key benefits to performing robotic assembly; chiefly, by allowing it to be adjusted to the needs of the robot and vice versa. Because the assembly is entirely autonomous and performed by a relatively low-cost robot, the structure needs to be able to be consistently put together under supervised conditions. The main strategy employed in the design of the structure is using compliance, or features that force alignment and connection. This allows for an amount of imprecision and uncertainties in position and placement to be adjusted for.

1.2.1 Robotic On-Orbit Manufacturing and Repair

On-orbit manufacturing has already begun in space from many companies. One of the earliest examples is Made in Space, who sent the first 3D printer into space in 2014 [38], and is now working on a project known as Archinaut, a robotic manufacturing and assembly system to aid in in-space construction of large objects [26]. Momentus Space has been a pioneer in in-space orbit delivery, developing Vigoride, a "charter" service to deliver satellites to specific orbits, then be available to refuel, reposition, repair, and de-orbit them as needed [21]. DARPA has also developed multiple on-orbit servicing projects, such as Phoenix [27], Robotic Servicing of Geosynchronous Satellites (RSGS) [31], and the Consortium for Execution of Rendezvous and Servicing Operations (CONFERS) program [9], all focused around service and maintenance of on-orbit satellites with robotic arms.

A report by IDA [5] emphasizes two benefits that on-orbit manufacturing gives to the space industry: building larger and building less rigidly. While this work does not look to building larger, it certainly takes advantage of the lower rigidity that is available by not needing to survive launch fully constructed. Launch loads, vibrations, and shocks are by far the greatest stresses that are put on a CubeSat. By skipping those, the CubeSat can be designed much simpler, allowing for ease of construction.

There have also been several proposals and discussions around smaller-scale on-orbit manufacturing and repair, such as a CubeSat spacecraft for telerobotic surgery, utilizing similar technology as Phoenix [25], a small swarm of CubeSats outfitted with robot arms to construct a larger satellite [14], or a 3U satellite with robot arms, designed to perform construction onboard the International Space Station (ISS) [16].

This project enters this space in different and important ways. First, this is the only project that strives to construct small satellites on orbit. Second, many of these on-orbit repair missions rely on using robots that are robust to a number of different satellite configurations for those they are repairing. By instead developing a CubeSat structure in conjunction with the robot, we remove many difficulties of needing to adapt to unknown or poorly compatible systems.

1.2.2   3D Printing on Satellites

Made in Space's 3D printer is not the only 3D printed material that has been to space; many satellites have been designed to utilize the technology. Actively 3D printing on orbit, such as the work done by Made in Space, or proposals for building projects in space, such as a parabolic reflector [40], is not the focus of this work, as the locker is designed to house structures pre-fabricated. More detail on the reasons behind this decision can be seen in Chapter 2.

There are many satellites that have been designed to be partially or entirely 3D printed. One of the earliest was RAMPART (Rapidprototyped MEMS Propulsion And Radiation Test), a 2U CubeSat whose main body and solar panel were 3D printed [22], although it never launched. Its direct descendent was PrintSat [8], a 1U satellite whose structure was fully 3D printed and plated in nickel. PrintSat unfortunately also never made it to orbit, as it was lost in launch failure [30]. The same people behind PrintSat also made KySat-2 [8], a 1U satellite that was launched in 2013. KySat-2 had multiple 3D printed parts on it, specifically the imaging system mounting. Another satellite was Tomsk-TPU-120 in 2016, a Russian satellite whose body was 3D printed. It was launched by hand from the ISS [11].

Although these all leveraged additive manufacturing, none of them had designs that would be impossible to construct out of other materials; most were simply technology demonstrations. A more unique example is MakerSat [15], a 1U CubeSat that was designed to be snapped together by an astronaut on the ISS after 3D printing the rails for it. This design could almost certainly only be made with 3D printing. Another unique structure design that was developed is called SnapSats, [32] which integrate electronics directly into the CubeSat boards. These boards are then snapped together by hand.

1.2.3   Compliant Design for Robotic Assembly

The main strategy that will be employed for the structure assembly are compliant design techniques. Compliant features are flexible mechanisms that deform elastically

to ease assembly of parts by guiding things into the proper position. Compliant design allows for us to simplify our robot and algorithms, as they increase the number of acceptable insertion configurations. These compliant features can be used both on the robot and on the parts being assembled.

A commonly found feature for a robot is a remote center of compliance [12], a device which causes parts being inserted into holes to slide and rotate into proper orientation when they experience external moments from improper placement. Another compliant feature is the ability for a gripper holding a part to slide. An example of this is if a robot is attempting to place an item in a precise location. If a wall is placed to form a corner, the robot should be able to push the item against it without dropping it, ensuring it is in the right location without needing extremely high precision.

On the structure, a compliant feature could be something like a button that only goes into a hole in one orientation or a latch that snaps around a part to hold it in place. Compliant design features heavily in the custom structure. These features are integral in creating a structure that is robust to minor flaws in alignment to ensure consistent, repeatable assembly.

1.3 Thesis Objectives and Organization

In this work, we analyze the set up for a Cartesian robot and custom structure, the testing, and the repeatability of assembly. We seek to:

- Determine the requirements for safe assembly

- Design a CubeSat structure that can be assembled by a robot

- Assess the time it takes the robot to assemble a full CubeSat

- Assess the reliability and repeatability of assembling the structure

With the success of this work in developing the CubeSat structure, a functional satellite can be assembled with a robot, a key step to assembly and deployment of

multiple variants of CubeSats on orbit. This thesis begins by detailing the requirements and design of the CubeSat structure (Chapter 2), then determining the safety requirements by performing a STPA (Chapter 3). The test procedure is then detailed (Chapter 4), the results are presented and discussed (Chapter 5), and final conclusions are made (Chapter 6).

Chapter 2

Approach

In this chapter, the approach for designing the structure and programming the robot is discussed. The requirements for the structure are created, and the resulting structure design is presented. The structure design considers different 3D printing materials and compliant design features. It is designed considering the expected forces during construction. Next, the robot test set up is presented, including the hardware and software utilized.

2.1 Structure

2.1.1 Design Requirements

CubeSat assembly on orbit requires structures that ensure compatibility with the robot and the low gravity environment. Requirements are developed for the CubeSat structure, listed and discussed in Table 2.1. The strategy is to consider the minimum capabilities of a robot to perform assembly, and modify requirements as necessary once the robot specifications matured.

Table 2.1: Requirements for the CubeSat structure and given rationales.

Requirement	Rationale
1. The structure shall be able to be manipulated by the robot. It shall be compatible with both a finger gripper and an electromagnetic gripper. The finger gripper requires a maximum part size of 4 cm, and the electromagnet requires a magnetic target on each part surface.	In development, it was not clear whether a finger gripper or a electromagnetic gripper would yield better results. It was determined that the structure should be compatible with both for comparative testing.
2. The structure shall be able to be assembled without fasteners such as screws or springs. It shall not have wires to be manually connected using the end effector.	It is certainly not unreasonable for a robot to install screws using compliant design [24] and with Cartesian robots [29]. However, the low gravity environment on orbit introduces several factors of risk that makes use of small fasteners undesirable. Losing a screw in the locker creates foreign object debris (FOD), which may cascade to failures later in assembly. It also would require more parts to be stored in the locker.
3. The success for the robotic assembly of each part shall have a significance level of 0.05 (5%) during the prototype phase.	The success of the robot to repeatedly perform assembly is crucial to becoming fully autonomous. During the prototype phase, where there is no feedback from cameras, it was determined a significance level, or the probability of it being random chance that the robot is succeeding at assembly, of 5% would be sufficient to be confident of continued performance with this design. If a structure failed to meet this criteria, it underwent redesign.
4. The robot shall be able to assemble the CubeSat without the aid of computer vision algorithms.	This requirement comes from the desire to make the assembly procedure robust once it is fully autonomous. Although computer vision will be necessary for closed loop control and verification, the robot should be capable of assembling a CubeSat without it.

5. The CubeSat structure shall be compatible with commercially available CubeSat boards.	One use-case for this project is to be able to have backup CubeSats on orbit for constellations. These constellations likely use boards that are of similar size to commercial ones.
6. The CubeSat structure shall be able to hold at least 6 boards.	A typical 1U CubeSat has 6 boards (command and data handling, electronic power system, batteries, communications, ADCS, payload)
7. Assembling the CubeSat structure shall automatically mate all electronics, including boards and solar panels. Doing so will not power the satellite. The structure shall have a mechanism to allow power to flow after assembly is completed.	The amount of precision required to attach wires from one board to another exceeds the abilities of the Cartesian robot. Power flowing through a partially assembled satellite is likely to cause electrical damage the boards.
8. Any hole where a peg must be inserted shall either have a radius 1.5 mm greater than the radius of the peg or it shall have a minimum of a 1.5 mm chamfer on all sides.	Through empirical testing, it was determined the highest minimum deflection of the Cartesian robot axes was the X axis with a deflection of 0.15 mm. A safety factor of 10 was placed on this based on initial testing results.

One notable exclusion to these requirements is for the constructed CubeSats to follow the Cal Poly CubeSat standard [10]. Because we are not planning on using P-POD launchers or going through rideshare programs, it was deemed unnecessary; the deployment system on the locker will be customized to match the needs of the structure and the locker itself. The final 1U CubeSat exceeds the standard by its outer dimensions, being larger by approximately 20 mm on each side. It is feasible to scale down the structure if a traditional deployer is necessary, although it would also need to be reformulated to survive launch loads fully constructed.

2.1.2 Materials and Method

In order for the structure to be constructed without fasteners, it must be able to mate with itself as it is being put together. Features that could allow this include

magnets, latches, and slots. Latches and slots, which require pliable material, make the use of 3D printing attractive. 3D printed material also offers many advantages over materials such as machined aluminum. First, it allows flexibility in the prototyping phase. Rapid prototyping allows for fast and efficient redesigns as problems arise. Second, it is less expensive than machined aluminum parts, supporting the low cost goals of the project.

There are various types of 3D printing, each of which results in different material properties. Fused filament fabrication (FFF) involves material being extruded and deposited in layers to create a solid. FFF printers have been used in space, such as on the ISS [4], using materials such as acrylonitrile butadiene styrene (ABS), polyphenylsulfone (PPSF), polycarbonate (PC), Ultem 9085 [38], and polylactic acid (PLA) [23]. The other type of 3D printing considered is selective laser sintering (SLS). SLS printers use a laser to sinter polymer powder into a solid.

In order to use a material on orbit, it needs to adhere to outgassing standards set by NASA and other space agencies to ensure the safety of electronics and lenses from captured gases inside structures. Material properties databases exist on both NASA [3] and the ESA websites [1]. Although many 3D printed materials have successfully used on orbit, outgassing is still a major concern. When FFF parts are constructed on Earth, it is possible for gases to become trapped in between layers [13] and cause the parts to fail. (As a note, FFF done on orbit or in a vacuum does not have this same issue, as there are no gases to become trapped.)

Several materials were examined for use with this project, looking at their structural strength, outgassing properties, and use on previous missions. The material trade study can be found in Table 2.2.

Table 2.2: Trade study between 3D printed materials, including structural properties, outgassing properties, and prior use on orbit

Material	Tensile Modulus [MPA]	Tensile Strength [MPA]	Outgassing	Precedent	Manufacturing Technique
Acrylonitrile Butadiene Styrene (ABS)	1681	33.9	Mixed – results of failure [13] and passing [28]	MakerSat [15][1], Plastic CubeSat [28]	FFF
Polyetheretherketone (PEEK)	3738	99.9	Passes	ESA CubeSats [6]	FFF
Polyamide 12 (PA12/Nylon 12)	1700	45	Unknown[2], but there is precedent for its use on orbit	Tomsk-TPU-120 [11]	FFF
Polylactic Acid (PLA)	2200	50.8	Passes [3]	None	FFF
ULTEM 9085	2200	72	Passes [33]	COSMIC-2 [2]	FFF
Windform XT 2.0	8928.2	83.84	Passes [39]	PrintSat, KySat2 [8]	SLS

Ultimately, it was decided to use ULTEM 9085 for the final satellite and PLA for prototyping. The best precedent for use on orbit can be found in ULTEM 9085 and in Windform XT 2.0. ULTEM 9085 was more attractive for this process due to its lower stiffness, allowing for a structure designed to bend and not break. ULTEM 9085 also has similar structural properties to PLA, which is easier to obtain and prototype with. All testing was done with PLA structures with 30% infill.

---

[1] The failure of ABS is from constructing the parts outside of vacuum and putting them in vacuum. MakerSat was 3D printed in a vacuum and thus does not have the same issue.

[2] While Nylon is in the NASA outgassing database as passing requirements, it does not specify if it is 3D printed. It is unlikely, as the other 3D printed materials in the database are marked.
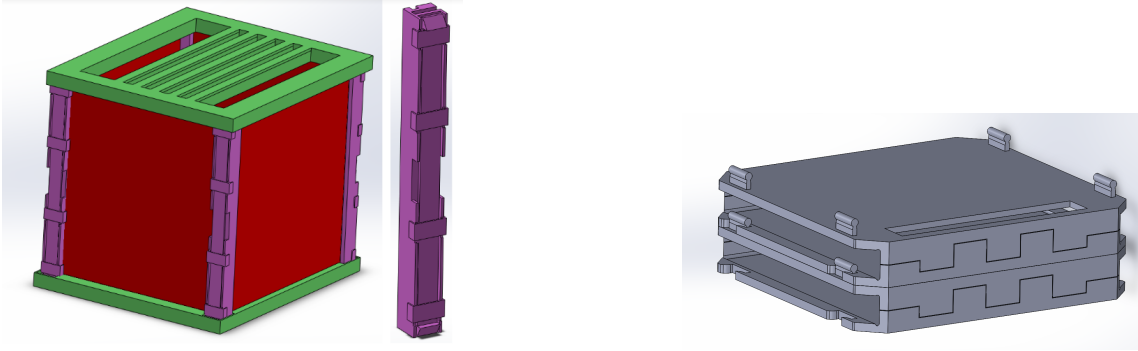
Figure 2-1: The design of two early satellite designs. They were both ultimately rejected because of their incompatibility with the robot. Revision 1 (left) utilized a spring-loaded rail system that was too small for the robot to actuate. Additionally, the "foot" at the base of the rails that held them in place would have to be prohibitively large to function properly. Revision 2 (right) utilized one-way buttons that were often too difficult for the robot to press together and were unreliable when assembled.

2.1.3 Rejected Prototypes

The structure went through several prototyping phases over the course of the project, each attempting different compliant designs. Because of 3D printing, these structures could be constructed quickly, tested, and redesigned as necessary. The two most developed ones prior to the design utilized in this thesis are shown in Figure 2-1. Both were ultimately rejected, either due to incompatibility with the robot or inconsistent performance in holding itself together.

2.1.4 Current Structure Design

The current structure, Revision 3, followed the principles set out by the requirements and the materials. The general design of the satellite is to have stacked layers of boards that are attached with cantilevered latches that can only be inserted one way.

Design

The Revision 3 CubeSat mockup is shown in Figure 2-2, both with and without solar panels. The structure is constructed via the method shown in Figure 2-4.
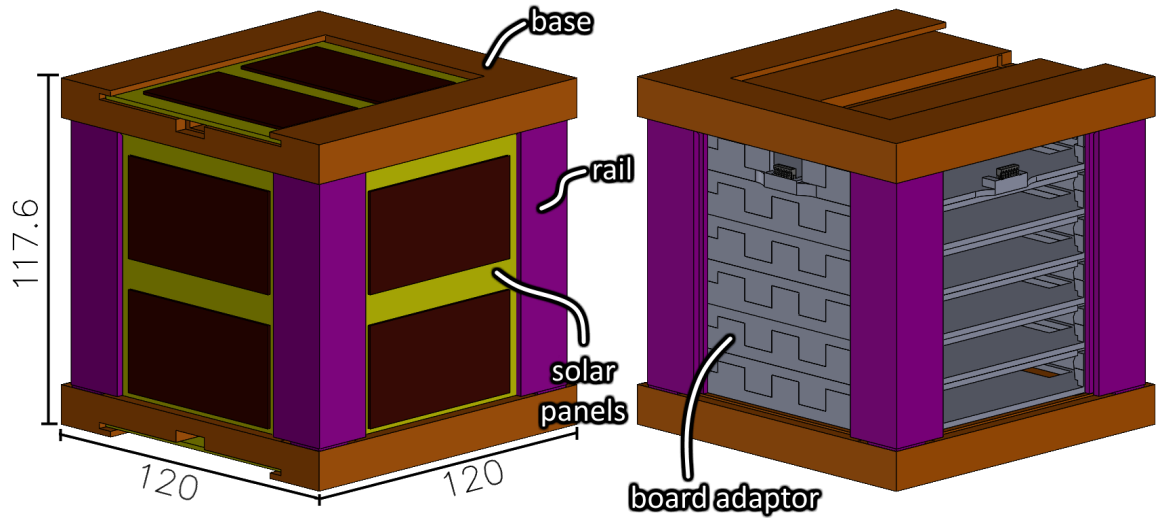
Figure 2-2: The design of the custom satellite structure. On left, there is the satellite with the solar panels installed. On right, there is the satellite without panels. The key parts are the bases (orange), the rails (purple), the board adaptors (grey) and the solar panels (yellow). Dimensions are in mm.

There are five main parts to the structure: bases (orange), rails (purple), board adaptors (grey), and solar panels (yellow). Within these, the bases have two types (the bottom and the top), and the adaptors have three types (normal, extended, and panel interface). Each part will be discussed individually and as a whole.

Holistically, the structure is capable of assembly by both an electromagnetic gripper and a finger gripper. Each part is placed top-down in this design, so an electromagnet on the end of the Z-axis can place each part without need for additional degrees of freedom. A finger gripper can hold each part and place them as necessary as well.

There are six adaptor boards, whose design can be found in Figure 2-3. There are no external fasteners holding them together. As seen in step three of Figure 2-4, each adaptor has a cantilever latch. The cantilevers slide over an outcropping in the lower board, and snap underneath it to secure the part in place. There is a cantilever and snap on each corner. A detailed view of these latches can be found in Figure 2-5. The calculations that were done to determine the dimensions of these latches can be
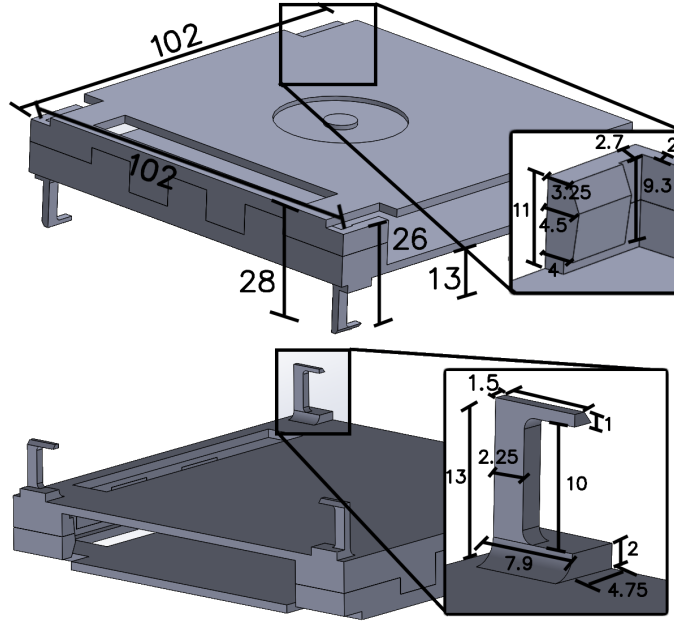
Figure 2-3: The adaptor boards, viewed from top and bottom. The corners mate into each other, allowing for the cantilever to slide over the outcropping. There is an indent shown in this diagram for the magnetic adaptor. All units in mm.

found in Subsection 2.1.4.

The adaptors additionally have rectangular holes to allow for electronic pass through. Each electronic CubeSat board will be modified or designed to use spring-loaded pogo pin connectors, which allow for electric connection when they come into contact. An example of pogo pins in action are shown in Figure 2-6.

There are two other variants on the adaptor board. One is shown at the top of the right image in Figure 2-2. There are small outcroppings on the top of this board that have electronic connectors on them. When the solar panels are inserted, they automatically plug into these connectors. The other variant on the adaptor board is one that is twice as tall, and internal height of 30 mm rather than 15 mm, used for taller CubeSat boards. It is otherwise identical.

The bottom and the top bases have similar designs to each other; the bottom is shown in Figure 2-7. The bottom contains holes in each corner of the same design as the adaptors, to allow for mating. There are chamfers on all sides of these holes.
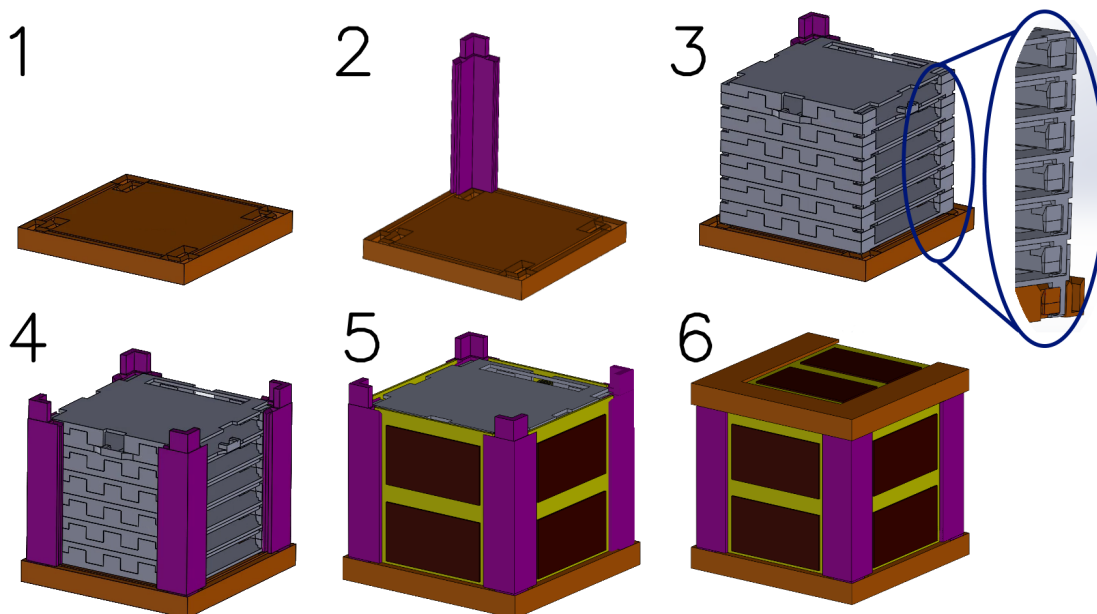
Figure 2-4: The six steps to performing assembly of the custom structure. Not pictured are the magnetic targets on each part.
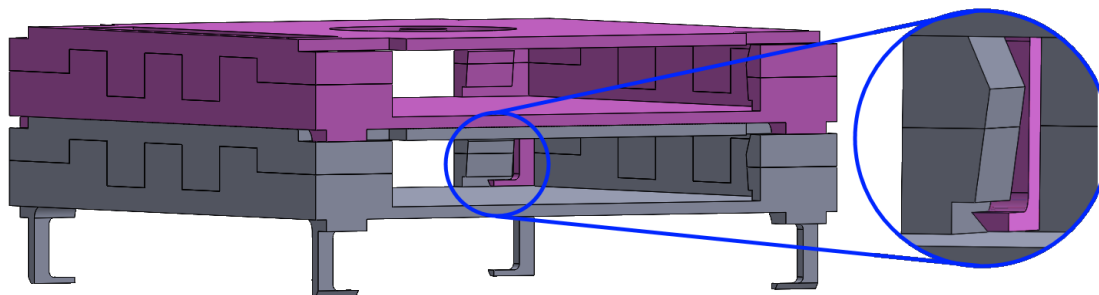
Figure 2-5: A detailed view of the latches in their mated position. The latch slides around the outcropping on the adaptor below to mate.
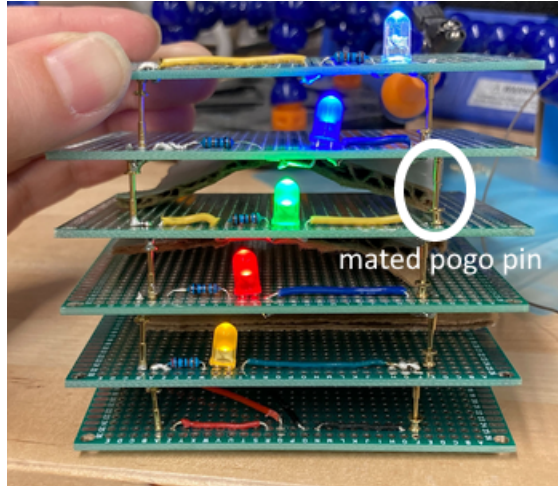
Figure 2-6: A demonstration of prototype boards with pogo pin connectors. These allow for contact transfer of current and data, eliminating the need for small wire connections or precise pin connections.

The top has cantilever latches in the same locations. Both of these bases also contain slots for each of the four rails, with similar chamfers and slots for solar panels.

The rails are shown in Figure 2-8. They slot into the base and top and are held in with friction from the top and bottom. They have outcroppings on each side to hold the solar panels in place. There are slight chamfers on the top of the rails to allow for the solar panels to slide in.

Structural Analysis

In order to size the cantilevered latches, a basic structural analysis was done. To first solve for the force that the overhang in the cantilever latch experiences when it is pushed over the outcropping, which has a designed deflection of 0.75 mm, Equation 2.1 is used.

$$\delta = \frac{PL^3}{3EI} \tag{2.1}$$

Where δ is the deflection, P is the force applied, L is the length of the cantilever, E is the Young's Modulus (same for both ULTEM and PLA), and I is the moment of
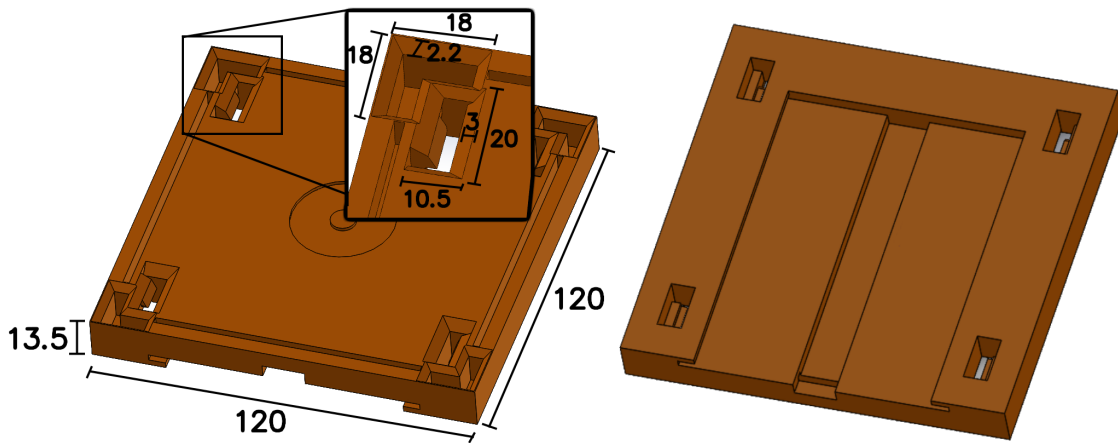
Figure 2-7: The bottom base, which has holes for the adaptors to mate to, slots for the rails, and slots for the solar panels. The top (not pictured) is the same, except it has latches instead of holes.
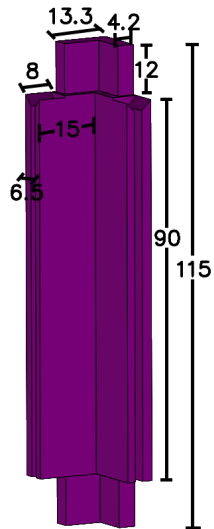
Figure 2-8: One of four rails for a CubeSat. It mates into the base and top by friction, and it has slots for the solar panels to slide into.

inertia.

Next, the bending stress was calculated using Equation 2.2.

$$\sigma_b = \frac{Mc}{I} \qquad (2.2)$$

Where M is the maximum moment (equal to PL), c is the half-side length, and I is the moment of inertia.

The values from this analysis can be found in Table 2.3. Holding a factor of safety of 1.5, both the ULTEM and PLA have positive ultimate safety margins. Testing was performed verify that the structure did not break when assembled by assembling the structures by hand.

Table 2.3: Values for the structural analysis of the cantilever latches. These values ensure the latches should not snap during normal insertion procedure.

Parameter	Value
End Deflection	0.75 mm
Beam Base	1.5 mm
Beam Height	2.25 mm
Beam Length	11 mm
E	2200 $\frac{N}{m^2}$
I	1.42e-12 mm^4
P	5.3 N
Max moment	0.058 Nm
Bending stress	30.7 MPa
ULTEM Margin	0.564
PLA Margin	0.104

2.2 Robot

2.2.1 Robot Test Set Up

The Cartesian robot used for this research is shown in Figure 2-9. The Cartesian robot was constructed in-house from COTS parts. The base is a custom frame and
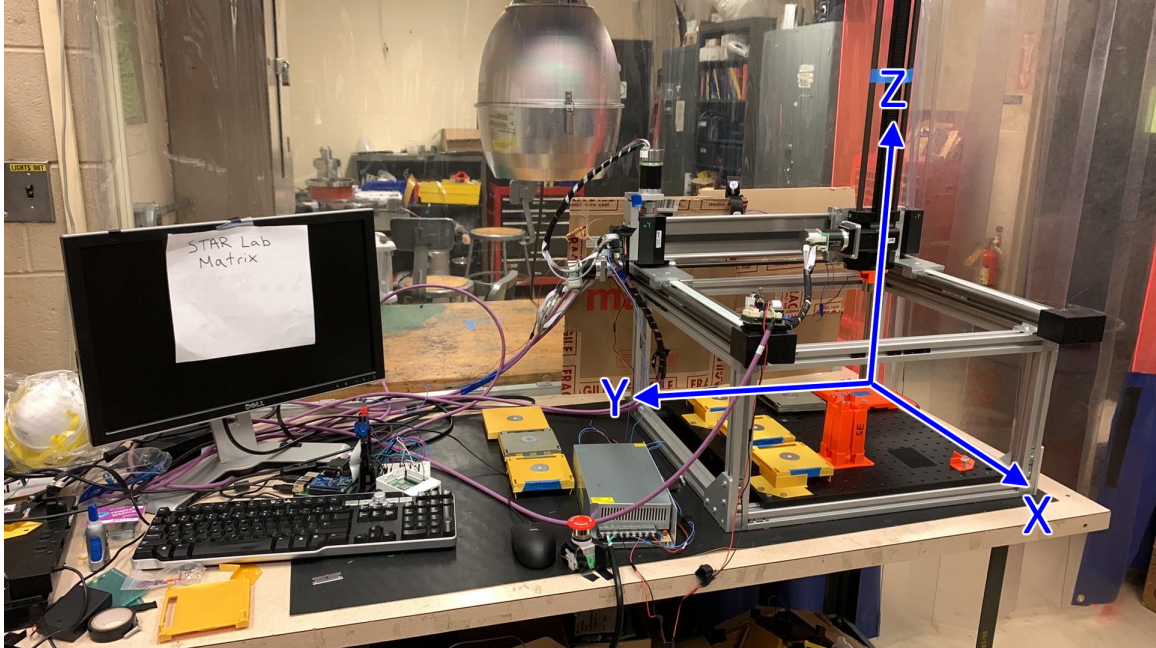
Figure 2-9: The set up for the study with the axes labeled. The gantry base contains all of the parts pre-aligned. The robot is powered by a power source, and is controlled by a Raspberry Pi, which communicates via a CAN network (purple cable).

threaded board for accurate alignment of CubeSat parts. Atop the base is a XYZ gantry robot from igus, headquartered in Germany. The gantry is controlled by three brushless DC motors made by maxon, headquartered in Switzerland. Each of these motors has a dedicated controller, called an EPOS, routing both the power and the data to the respective motors. Each EPOS receives its commands from a master controller, a Raspberry Pi, through a CAN network, a robust serial bus system for networking devices. The gripper is affixed to the end of the Z axis, and can be commanded to move to any point in 3D space within an accuracy of approximately 0.15 mm.

The gripper is a simple electromagnet which is commanded by a second Raspberry Pi. The electromagnet has only two states, on and off. The whole assembly is powered by a 12 V external power source, which can provide 50 A.

2.2.2 Robot Programming Principals

The master controller runs scripts that are written in Python, utilizing modified versions of the commands that were provided with the maxon motors and controllers. Commands included "move to target position" and "return current position."

In terms of control, each motor has an individual PID controller that was tuned according to each motor's properties. They also have internal sensors to track their position over time and report if the estimated position accumulated an excess of error. The implemented motion commands worked with a timeout system: the robot is given a position to move to and a time to get there. If the robot reaches its target before the timeout occurred, it completes the command and moves to the next one. If the timeout occurs while the robot is still in motion, it keeps moving. If the robot is not in motion when a timeout occurs, it checkes if it is in the correct position. If not, the robot concludes it has encountered an error. The most typical error that causes this is if the controller's estimate for its current position accumulated too much uncertainty. If this happens, the robot has the error reset and it was given the motion command again. This repeats until the robot reached the desired position.

The robot reports back its position, velocity, and current draws throughout its motion. The position values are given in mm for the coordinate system shown in Figure 2-9, the velocity values are given in mm/s, and the current draws are given in amps. These are collected for diagnostic reasons to ensure the gantry was following the given commands and was not experiencing unexpected spikes or drops in current draw. All values were within expected parameters for the entirety of the tests.

2.2.3 Path Planning Algorithms

Generally, the path (as further described in Chapter 4) is simple for this assembly; there are no unknown obstacles, and the parts are all in known locations. In theory, the path could fully be written by hand with no calculations. However, path planning

is still valuable for future iterations of the robot system, as rapid replanning given unforeseen obstacles is key for a fully autonomous system. Therefore, a simple algorithm was developed for this study, although it was not analyzed in detail, which is an item for future work.

Some of the most widely used path planning algorithms for Cartesian robots are A*, D* Lite, RRT, and RRT*. RRT, or rapidly-exploring random trees, and RRT*, the optimal version of that algorithm, both function by creating search graphs and finding paths within them. They sample the state space and create connections between each of the sampled points, continuing until the goal is found. RRT returns unoptimal paths, which would waste a lot of time for a simple state space such as this one. RRT* is optimal, but much more computationally expensive. The main reason we use neither is because the bulk of of their computation is used for sampling, which, while useful for state spaces with unknown routes, is unnecessary for the controlled robot environment.

A* and D* Lite both require the state space to be fully known before being run. A* is a best first algorithm that utilizes a weighted graph of the possible locations, calculating the path to take according to the heuristic in Equation 2.3.

$$f(n) = g(n) + h(n) \tag{2.3}$$

Where $g(n)$ is the cost of the path so far, and $h(n)$ is an estimated heuristic to the goal.

A* is simple and well-studied, but it does not scale well to a 3D state space. Additionally, A* must be completely restarted if an unknown obstacle is added. As stated, the test set up is not currently robust to a changing environment, but we would want the path planning on the fully autonomous robot to be robust to things such as broken parts creating new obstacles (see Chapter 3).

An alternative method is D* Lite [17], a path planning algorithm that is an ex-

tension from Lifelong Planning A*, a variant of A* which is calculated incrementally. Like A*, a heuristic is used to estimate the path to the goal. However, D* Lite stores all path planning calculations. If, while following the calculated path, it encounters an obstacle, it is able to rapidly readjust to avoid it without needing to fully rerun. D* Lite has been implemented in 3D space [7].

D* Lite is selected for this CubeSat robotic assembly demonstration. It was implemented to find a path to place each part into the final CubeSat. The outputs were then adjusted manually to account for compliant assembly techniques and robot imperfections (see Chapter 4).

2.2.4 Feedback Control

Although there is internal closed loop control within the motion of motors, no feedback control is currently used to modify the commanded position given by the path planning algorithm. Similar to how the path planning would need to be implemented in future work on a fully autonomous version of this system, feedback control would also need to be added for robustness to the assembly process. An example of such feedback could be a camera that reports the alignment of parts before pressing them together, or that reports unforeseen obstacles as inputs to the path planning algorithm.

Chapter 3

System Safety

In this chapter, a Systems Theoretic Process Analysis (STPA) [19] is performed. This is done by first identifying the system boundary, both on the test bed and on orbit. Next, a hierarchical safety control structure is identified. From this, unsafe control actions are found, and mitigation plans are examined.

3.1   Overview

In order to ensure the safe operation of the system, a Systems Theoretic Process Analysis (STPA) [19] is performed. A STPA uses process models to determine control actions between individual parts of the system that can lead to the system entering an unsafe state. Determining the combination of factors that can lead to these states and then preventing them is key to a successful mission.

By "unsafe" state, we refer to states that put any part of the larger system in danger – the robot, the structure, or the operators. Because the same robot will be used both in the lab and in the autonomous spacecraft, the safety design must accommodate both contexts, as designing for only one would inevitably lead to design choices that would adversely affect the other.

As a note, this safety analysis was done after certain pieces of hardware were pur-

chased, and thus some inconsistencies exist between the recommendations presented at the end of this analysis and what was constructed. One example is that the EPOS controllers are unable to have their internal estimate of their location updated manually, making the use of a third party limit switch system difficult. This safety analysis was done ignoring limitations from specific pieces of hardware in order to give firmer recommendations for future hardware purchases and modifications to the system. Notes are included where any inconsistency occurs. The analysis also includes parts that do not exist in the current system but may in the future, such as using a finger gripper rather than an electromagnetic one. Such a gripper would actuate to open and shut configurations and rotate in one or more axes. The electromagnetic gripper is hard mounted to the Z axis and can only translate linearly.

An example task list for the robot includes sequential actions such as:

1. The robot is given a command to assemble a satellite with a given set of boards.

2. The required 3D printed boards are delivered to the robot work area, either by a secondary system on orbit or by an operator on the test bed.

3. The robot picks up the base board and places it in the assembly area, where it is secured.

4. The robot picks up the next part and places it in the proper location on top of the partially constructed satellite.

5. The robot aligns the part, utilizing the compliant design features.

6. The robot presses the part into place, connecting it with the in progress satellite.

7. Repeat steps 4-6 until the satellite is completed.

8. If on orbit, the satellite is deployed. If on the test bed, the operator inspects and deconstructs the satellite.

Table 3.1: Parts of the system in the test bed system boundary.

Cartesian Robot (gripper, motors, controllers, master controller)
Satellite parts
Human operator

Table 3.2: Parts of the system in the orbital system boundary.

Cartesian Robot (gripper, motors, controllers, master controller)
Satellite parts
Autonomous locker spacecraft
Satellite deployer

3.2 System Boundary

We define the parts of the system boundary on the test bed in Table 3.1 and the parts of the system boundary on orbit in Table 3.2. On the test bed, the human operator is used to monitor the robot's performance and reset the constructed satellites between tests. Once on orbit, all previously human tasks are performed autonomously.

3.3 Losses, Hazards, and Requirements

The primary losses are in Table 3.3. We note that L-1 and L-2 are specific losses in the context of the first system boundary. The robot being damaged is not necessarily considered a loss once on orbit. As long as it remains operable, it does not always cascade to a loss of mission.

From these losses, we reach the hazards found in Table 3.4. The most important hazards to analyze are H-1 and H-4. H-1 leads to all three of the identified losses, making it crucial to avoid. The robot being uncontrollable is defined as any situation

Table 3.3: The three primary losses.

L-1: Operators are injured
L-2: Robot is damaged
L-3: Loss of the mission

Table 3.4: The four system hazards.

H-1: Robot is uncontrollable [L-1, L-2, L-3]
H-2: Robot exceeds safe operating envelope for environment [L-1, L-2, L-3]
H-3: Operator appendages are near moving parts [L-1, L-2]
H-4: Robot does not maintain proper gripping strength on parts [L-2, L-3]

where the robot does not follow the expected performance of the commands that are given to it, whether by an operator or autonomously. H-4 is a hazard that applies to both the magnetic and finger grippers; the electromagnet may not trigger, leading to it not picking up or letting go of the part, or the finger gripper may squeeze too little or too firmly. Tight squeezing could lead to damage that could break the satellite parts. While on orbit, this leads to mission failure. The robot is unable to retrieve free-floating parts, which become unpredictable obstacles. Moreover, if either gripper does not actuate after placing or aligning a part and moves to press it in, the existing boards or the board to be added could be damaged, leading a similar scenario.

These hazards lead to technical system safety requirements found in Table 3.5.

The overall management or organizational requirements are directly related to expanding the system boundary to include the prototyping phase. We develop the following management requirements:

1. Safety considerations must be involved in technical decision making. No requirement for safety may be impeded by the influence of money or time.

Table 3.5: The four technical system safety requirements.

R-1: Robot must always respond to autonomous or operator commands. [H-1]
R-2: Robot must not exceed safe operating speeds [H-2]
R-3: Operator appendages must not be able to contact moving parts [H-3]
R-4: Robot must maintain proper gripping strength on parts. [H-4]

2. Safety analysis must be done in tandem with requirements development.

3.4   Hierarchical Safety Control Structure

The simple and refined hierarchical safety control structures for the robot prototype (with operator in the loop) are shown in Figures 3-1 and 3-2. A version of the refined structure for a finger gripper can be found in Figure B-1 in Appendix B.
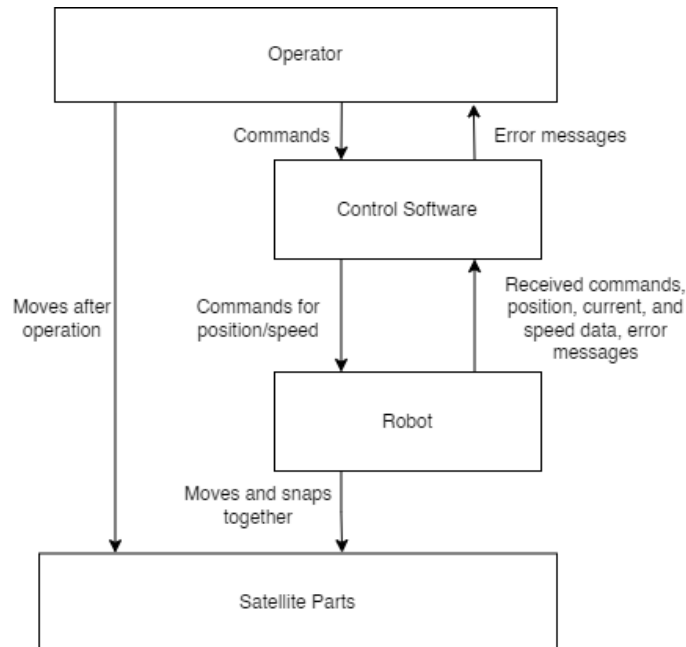
Figure 3-1: A simple version of the robot control structure on the test bed, identifying the major parts of the system boundary.

The simple hierarchical safety control structure is developed by considering the
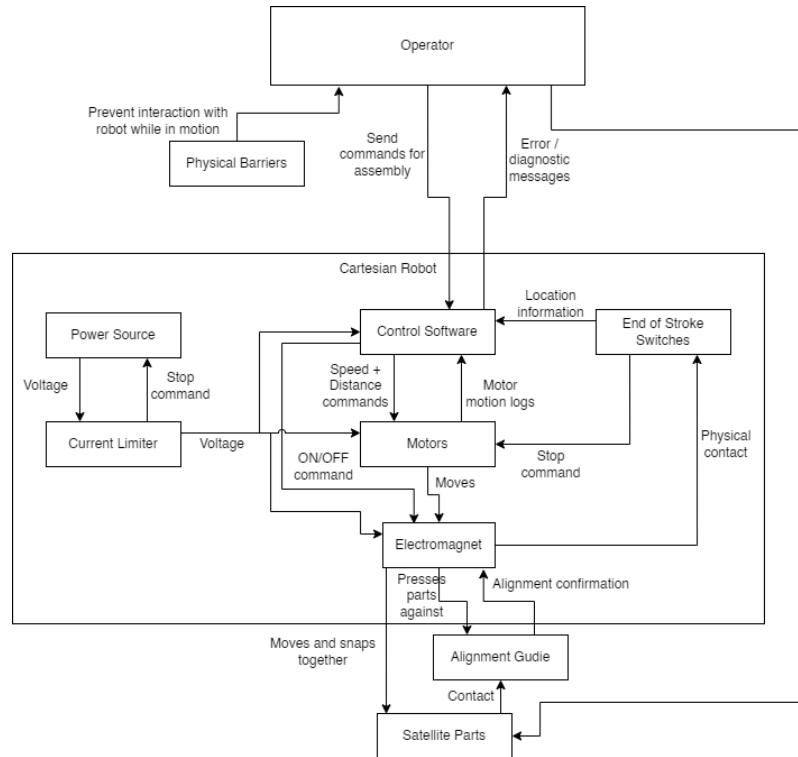
Figure 3-2: A refined version of the robot control structure on the test bed. This version is for the electromagnetic gripper.

basic needs for robotic assembly. It shows a linear safety control structure; the operator only directly interfaces with the control software and with the satellite parts after assembly takes place. The control software talks with the robot, commanding it to pick up and manipulate satellite parts.

By analyzing these system boundaries, potentially unsafe interactions are separated out and defined, and additional control features are added to create the refined diagram in Figure 3-2. We break the robot out into its two main parts: the motors that move it around and the gripper that manipulates parts. Both directly interface with the control software which is commanded by the operator or autonomously. There are a number of additional features added as controls are identified. For one, a physical acrylic barrier that is able to be moved will prevent an operator from getting too close to moving parts during operation, but can be removed after operation to perform satellite resets. Second, end of stroke switches are able to both stop the

robot before it has a collision as well as provide feedback to the control software about where the robot currently is located, as, otherwise, it only calculates this based on odometry data from the motors.[1] The motors, controllers, and gripper, which have a shared power source, have a current limiter to prevent over voltage damage.

Finally, the satellite assembly process is aided by alignment guides, small pieces of plastic that show where the corners should be, to confirm proper alignment before the gripper attempts to connect two satellite parts, preventing damage to the 3D printed structure and improper electronic alignment. Detailed analysis of this compliant design can be found in Chapter 2.

3.5 Unsafe Control Actions (UCAs)

Each control interaction between systems is analyzed to find the following unsafe control actions (UCAs). There are separate UCAs for the operator and the autonomy, and they are listed in Tables 3.6 and 3.7.

Resulting operator constraints:

1. The robot shall not begin motion into area where there are other objects in the way (e.g. partially constructed satellite, other satellite parts, foreign objects). [UCA-1, UCA-8, UCA-9, UCA-12]

2. The robot shall be able to handle multiple "start" commands at once. [UCA-2]

3. The robot shall have current monitors to check for proper electric flow when powered on. [UCA-3]

4. The robot shall not move if physical barriers are not in place. [UCA-4, UCA-11]

5. Operator training shall inform proper use of emergency stop to prevent damage to robot and user. [UCA-5, UCA-7]

---

[1]Such switches are incompatible with the controllers currently selected, but the controller software has been modified to mimic the performance of these switches by using their collision detection.

Table 3.6: Unsafe control actions, as performed by the operator.

Control Action	Not providing causes hazard	Providing causes hazard	Too early, too late, out of order	Stopped too soon, applied too long
Assembly start command	N/A	**UCA-1**: Operator provides start command when assembly path is not clear. [H-2] **UCA-2**: Operator provides start command when robot is already in motion. [H-1] **UCA-3**: Operator provides start command when robot is not fully or improperly powered. [H-1]	**UCA-4**: Operator provides start command before replacing physical barriers [H-3]	N/A
Assembly emergency stop command	**UCA-5**: Operator does not provide emergency stop command when gripper enters unsafe location. [H-1]	**UCA-6**: Operator provides emergency stop command when robot is not in motion. [H-1]	**UCA-7**: Operator provides emergency stop command after conjunction has already occurred [H-1, H-2]	N/A
Moving satellite parts	**UCA-8**: Operator does not reset satellite parts to the proper locations after assembly. [H-2] **UCA-9**: Operator does not move satellite parts that are in a collision path. [H-2]	**UCA-10**: Operator moves satellite parts without disengaging the gripper. [H-2, H-3]	**UCA-11**: Operator moves satellite parts before robot stops moving by removing the physical barrier. [H-3]	**UCA-12**: Operator moves satellite parts to the incorrect position. [H-2]

6. Robot shall be tolerant to receiving stop commands when not in motion. [UCA-6]

7. If finger, the gripper shall autonomously open if an external force is applied. [UCA-10]

8. If finger, the gripper shall be able to be opened manually. [UCA-10]

9. If electromagnetic, the maximum strength of the magnet shall not be such that manual removal of parts is impossible when applied. [UCA-10]

10. If electromagnetic, the electromagnet shall be able to be powered down manually. [UCA-10]

Table 3.7: Unsafe control actions, as performed by the control software.

Control Action	Not providing causes hazard	Providing causes hazard	Too early, too late, out of order	Stopped too soon, applied too long
Distance commands (move gripper to coordinate)	**UCA-13**: Control software does not command distances as calculated by the path planning algorithm or commanded by the user. [H-1]	**UCA-14**: Control software provides a distance command that would place the gripper beyond its stroke. [H-1, H-2] **UCA-15**: Control software provides a distance command that would cause the gripper to intersect the assembled satellite. [H-1, H-2] **UCA-16**: Control software provides a distance command that would cause the gripper to still be in motion when the battery is depleted. [H-1]	**UCA-17**: Control software does not provide motion command quickly enough to retrieve dropped part. [H-2]	N/A (Distance commands do not have a duration).
Speed Commands	**UCA-17**: Control software does not provide a speed command as calculated by PID controller [H-1]	**UCA-18**: Control software provides a speed command such that it is unable to stop it before a collision. [H-1, H-2]	**UCA-19**: Control software provides speed command after motion is already in progress [H-1]	N/A
Gripper commands	**UCA-20**: Control software does not provide a grip command when attempting to move a part. [H-1]	**UCA-21**: Control software for finger gripper provides an excessive "close" command that causes the part to shatter. [H-4] **UCA-22**: Control software provides an insufficient amount of force that causes it to drop the part. [H-4]	**UCA-23**: Control software provides grip command before it is in the proper position. [H-1, H-2] **UCA-24**: Control software applies "open" or "magnet-off" command before part is fully placed. [H-1, H-2] **UCA-25**: Control software applies "close" or "magnet-on" command before gripper is in position. [H-1, H-2] **UCA-26**: Control software applies "close" or "magnet-on" command when it should have applied "open" or "magnet-off" command, or vice versa. [H-1, H-2]	**UCA-27**: Control software stops applying grip command before part is placed. [H-1, H-2]

Resulting constraints:

1. Control software shall command exactly as is calculated. [UCA-13, UCA-17, UCA-20]

2. The robot shall not begin motion into area where there are other objects in the way [UCA-14, UCA-15]

3. The control software shall take obstacles into account when issuing commands. [UCA-14, UCA-15, UCA-18]

4. The controller shall not issue commands when the battery is critically low. [UCA-16]

5. Retrieval commands shall override normal path planning commands. [UCA-17]

6. The robot shall be able to handle multiple speed commands at once. [UCA-19]

7. If finger, the gripper shall have force sensors to verify grip strength that was commanded. [UCA-21, UCA-22]

8. If electromagnetic, the gripper shall have external sensors to verify its state [UCA-22]

9. The gripper shall be able to verify its state before moving. [UCA-23, UCA-24, UCA-25, UCA-27]

10. The gripper shall not be able to operate if the robot is in motion. [UCA-23, UCA-24, UCA-25, UCA-27]

11. The gripper shall be tolerant to commands for the state it is already in. [UCA-26].

3.6 UCA Scenarios and Recommendations

We analyze scenarios that could lead to the most concerning UCAs, and provide recommendations. We also discuss test bed implementations that follow these recommendations.

3.6.1 UCA-1: Operator provides start command when path assembly is not clear

Scenario 1-1: The operator is improperly trained on what the assembly path is. There are multiple boards that are involved in CubeSat construction, and not every one is used with every satellite assembled. A poorly trained operator may not know that a certain part is in the assembly path if they are unfamiliar with all the possible paths.

Recommendation: Mark all assembly paths visibly on the gantry. This can be done by marking a brightly colored line anywhere the robot is expected to move in any of its operations.

Implementation: During assembly tests of individual parts, blue tape was used to denote expected paths. Once assembly for the full satellite began, however, it became impractical to mark paths, as the entire base of the gantry was being used. Instead, the order that things would be assembled was marked to ensure that the calculated path would not run into other parts.

Scenario 1-2: The operator believes commanded path will not intersect with assembly path when it will. Although the procedure may say that operators shall fully clear the robot parts before beginning the robot motion, if this takes an excessive amount of time, the operators may not perceive it as necessary. Even if the operator knows a part is in the motion path, if they expect the robot to go above it, they may not perceive moving it as worth their time.

Recommendation: The gripper should either have a sensor on it that can detect if it is about to hit something or there should be a monitoring camera that will issue an emergency stop command if it sees the gripper is about to have a collision.

Implementation: The structures that are currently being used are cheap and easy to replace, so effort was not yet put into implementation of this recommendation. However, a camera has been chosen to make this autonomous in future work.

3.6.2 UCA-5: Operator does not provide emergency stop command when gripper enters unsafe location. [H-1]

Scenario 5-1: The operator does not believe the gripper is in an unsafe location. Similar to scenario 1-2, if the operator believes the gripper will pass over or to the side of a part, they may not press the emergency stop command.

Recommendation: Same as scenario 1-2.

Implementation: Same as scenario 1-2.

Scenario 5-2: The operator is unable to provide emergency stop command. Such scenarios could occur if the emergency stop button does not instantly provide a stop (for instance, many emergency stops are incorrectly wired such that power is still flowing through the system for seconds after the emergency stop is pushed), or if the emergency stop is not located near the operator. This could occur if the operator sends a remote command to the robot and is unable to watch it, or if the operator is preparing for a next test.

Recommendation: All emergency stops should be tested to ensure that they stop the robot immediately. Additionally, if the operator station is not immediately adjacent to the robot, a second emergency stop should be routed to the operator's station to allow for remote stopping.

Implementation: There is only one operational station, which is immediately adjacent to the emergency stop. The emergency stop was tested and performs instan-

taneously.

3.6.3 UCA-10: Operator moves satellite parts without disengaging the gripper. [H-2, H-3]

Scenario 10-1: The operator cannot get the gripper to disengage. This may occur if the operator issues an emergency stop command for the motion, such that the command to disengage the gripper does not occur. If the operator is in a rush, they may attempt to force an actuated gripper open to remove the part quickly or pull the part off the electromagnet. Additionally, the gripper may be unable to disengage due to a hardware failure, such as the gripper becoming overworked and no longer being able to actuate. It could also be caused by a software bug that causes the gripper to stop receiving open/magnet off commands.

Recommendation: The software for both types of grippers should be able to open the gripper/turn the magnet off on command. They should also be able to perform a full reset to remove any commands that are unable to be overwritten. A finger gripper should be able to be taken apart when in a "stuck" state in order to safely remove parts and diagnose issues. An electromagnetic gripper should be able to be powered down via the hardware.

Implementation: The electromagnetic gripper is able to be powered off manually both through software and hardware.

Scenario 10-2: The robot has run out of power and the gripper cannot function. This is similar to scenario 10-1, but the status of how firm the gripper is holding onto the part is unknown, as well as how manual motion may be possible. This scenario is specific to a finger gripper, as an electromagnet is off if there is no power.

Recommendation: Instruct operators to charge all batteries before attempting to force the gripper in any way. Additionally, as was recommended earlier, the gripper should be easy to take apart to retrieve parts in scenarios such as this.

Implementation: Not applicable, as an electromagnet is being used.

3.6.4 UCA-11: Operator moves satellite parts before robot stops moving by removing the physical barrier. [H-3]

Scenario 11-1: The operator sees that the robot has performed an unsafe action and the emergency stop is not functional. The operator believes the best course of action to protect the robot and the parts is to interfere themselves.

Recommendation: The operator should be trained to put their own safety above the robot's and should not personally interfere. Additionally, the emergency stop should have redundancy in the event that one does not function.

Implementation: All operators have been trained, with emphasis on the low cost of the prototype structures.

Scenario 11-2: The operator believes the robot has finished its motion, but it has not.

Recommendation: The system should have a auditory "start" and "stop" tones, as well as a LED that changes color depending on if the robot is in a motion scenario or not. Both of these help the operator to determine when the robot is moving.

Implementation: The robot controllers have LEDs that indicate their status, which all operators have been trained on – blinking green for waiting for commands, solid green for running commands, and solid red for error states.

3.6.5 UCA-14: Control software provides a distance command that would place the gripper beyond its stroke. [H-1, H-2]

Scenario 14-1: The software has an incorrect perception of where the gripper is. The distance command it gives would be valid if it was correct.

Recommendation: End of stroke switches should exist to prevent the robot from crashing into the end of the rails, as well as to update the software with the position of the gripper. Additionally, when this occurs, the software should replan to prevent the robot from missing steps of assembly.

Implementation: The controllers being used have software implemented to set the maximum allowable follow distance, meaning, if it loses localization by a set amount, the motors automatically shut down. Unfortunately, it is currently not possible to update the controller location with an external limit switch. Options in the case of this error: one, the controller can be reset, which will cause it to use its last known state as its current position. This generally works well, as the motions for assembly do not require high precision. The robot is then are given the previous command again. The second option takes advantage of the internal collision detection software to mimic a limit switch. The robot can be commanded to move to the side at a low speed to prevent damage and, if it detects a collision, the "home" of the robot for that axis can be reset to its current location. Future choices of controller may consider swapping to controllers that can utilize limit switches.

Scenario 14-2: An unauthorized agent hacks into the system and provides rogue commands in an attempt to disrupt assembly.

Recommendation: Several failsafes can be put in place to monitor rogue commands. This situation can apply both on-orbit or on the ground. On the ground, the robot should be able to be removed from the network to prevent unauthorized access, and additional cyber security measures can be placed on the operator controls, such as only accepting them from a local computer. While on orbit, the robot is chiefly being controlled autonomously, so the ability for manual controls to be sent, other than halting all assembly, would likely not be built into the system. An additional strategy could be to simply shut down operation if the amount of of remote commands exceeds a set threshold or sequence.

Implementation: This was determined to be out of scope for the current stage of the project, but will be added to future work.

3.6.6 UCA-18: Control software provides a speed command such that it is unable to stop it before a collision. [H-1, H-2]

The causes and recommendations for this scenario is the same for UCA-14, only it incorrectly calculates its speed.

3.6.7 UCA-21: Control software provides an excessive grip command that causes the part to shatter. [H-4]

Scenario 21-1: The gripper incorrectly calculates how much grip strength it is applying to the piece and continues to apply more.

Recommendation: For the finger gripper, this could occur when it is lifting the gripper or pressing it into place. For the electromagnetic gripper, this can only occur when it is pressing it into place. A finger gripper shall have a pressure sensor, either included in the gripper or added by the user, on its fingers to verify the amount of pressure it is applying. The pressure sensor threshold shall take precedence over the command. Additionally, on the test bed, a pressure sensor can be placed on the assembly area to similarly verify the pressure being applied.

Implementation: The finger gripper sensors are not applicable, as an electromagnet is being used. The pressure sensor on the test bed shall be included in future work.

Scenario 21-2: The gripper is unable to stop the "apply grip" command, leading to too much pressure being applied.

Recommendation: The "apply grip" command should be programmed in a way that it has a hierarchy shut down to it, related to the pressure sensor as previously

discussed. The pressure sensor should have a handshake protocol with the gripper, and should be able to trigger a shutdown of the autonomous software if it doesn't respond to these handshakes.

Implementation: Not applicable, as an electromagnet is being used.

3.6.8 UCA-24: Control software applies "open" or "magnet-off" command before part is fully placed. [H-1, H-2]

Scenario 24-1: The software loses localization on the gripper and incorrectly determines its position.

Recommendation: Hard stops shall be placed in the corners of the assembly area that can aid in the robot guiding the parts into place. For example, when finding the correct X-Y position of a part, it should have a corner that it presses the part against to ensure it has found that correct orientation. The system can have a secondary confirmation of its position. If it ever cannot find the stop when it thinks it should, the robot can re-localize itself. Only after confirming its position in this way should it apply an "open" or "magnet-off" command. Additionally, all parts shall be designed in a compliant way that allows for corrective commands to ensure alignment.

Implementation: Initially, a large hard stop was implemented in the corner of the assembly area. It was designed that every part needed to be re-oriented against it before assembly, by pressing against it and dragging the part down. However, through testing, it was discovered that the friction from this hard stop caused the robot to enter an error state. Modifications were made to make much smaller alignment jigs, as well as leveraging the rails as jigs, to prevent this. A more detailed description of the assembly technique is discussed in Chapter 4.

Scenario 24-2: There is a race condition in the software leading to simultaneous commands of motion and opening.

Recommendation: The software shall not allow for simultaneous "move" and "place"

commands. The only simultaneous commands shall be "move" commands on all axes and "speed" commands.

Implementation: This was implemented. The command to actuate the magnet and move the robot are completely separate.

Chapter 4

Robot Testing

In this chapter, the study for analyzing the robotic assembly of the CubeSat structure is presented. The procedure for the test is described in detail, including the way assembly for each part will be approached. The criteria for success and failure are given.

4.1   Study Design

This study was designed to test the capabilities of both the robot and the structure. The robot needs to have sufficient capability for repeated assembly of CubeSats, and the structure needs to be able to be reliably put together by the robot. As stated preciously, all testing is done open-loop for initial feasibility considerations; a closed loop verification will be added to future work.

The layout of the testbed can be seen in Figure 4-1. Please note that the difference in part color is a relic of filament availability; all parts are made of PLA and have the same structural properties.

Each adaptor has tape (in blue) holding it together. This is because the clamshell is designed to be epoxied shut after the electronic board is inserted on the ground, prior to launch. Because the electronics are not yet included, the adaptors needed to
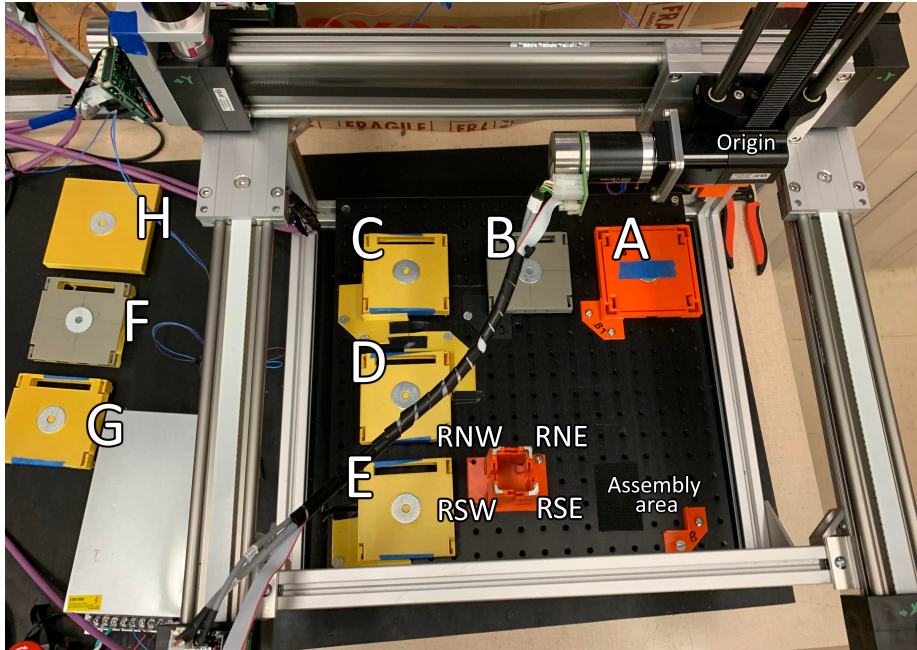
Figure 4-1: The test bed with each part labeled. A is the bottom, B-F are the adaptors, G is the top, and RSE, RNE, RNW, and RSW are the rails. The gripper is in its starting position as well, at the origin. The assembly area is in the lower right with the Velcro (as described in Section 4.2.1.)

be affixed together. Each non-rail part has an inset washer superglued or taped to the center of it to allow for manipulation by the gripper. The washer is larger than the contact area on the gripper to allow for compliant sliding when the part is being placed, as well as maximum grip strength. The rails have similar slivers of washers glued to their tops, which are shaved down to be fully contained within the surface of the rail and thus able to be inserted into the top when the time comes. These magnetic surfaces are smaller than the magnet, and thus are less easily grabbed and manipulated (see Chapter 5). All parts have custom alignment jigs to center the washer on a specific coordinate to ensure that each test has the same starting parameters. The operator is expected to place the part perfectly each test by pressing it to the corner of its alignment jig. The gripper begins at its home position, the upper right corner, before each test.

For each trial, the part being examined in the assembly procedure is placed in

position 20 times, with an operator disassembling that specific part in between each trial and inspecting it for damage. If the part is damaged, it is replaced. Damaged parts are tracked and logged.

4.2   Procedure

The assembly procedure is:

1. Place bottom (A)

2. Place rail (RSE)

3. Place adaptor (B)

4. Place adaptor (C)

5. Place adaptor (D)

6. Place adaptor (E)

7. Operator places adaptor F and G into adaptor C and D's alignment jigs.

8. Place adaptor (F)

9. Place adaptor (G)

10. Place rail (RNE)

11. Place rail (RNW)

12. Place rail (RSW)

13. Place top (H)

Figure 4-2: The procedure for installing the bottom. First, it is brought to the assembly area, where it may be slightly askew (due to incomplete grip in the magnet, improper initial placement, or other anomalies). It is aligned using the alignment jig. It is then pressed in, engaging the Velcro.

The solar panels would be inserted between steps 12 and 13 in a full assembly, but their insertion is not included for these tests, as it is impossible to lift them from the top with the current implementation of the magnetic gripper (this is discussed in more detail in Chapter 6). Details and strategy for each of these steps are in sections 4.2.1 through 4.2.5.

4.2.1 Place bottom

Placing the bottom only requires the robot to move it from the starting position to the assembly area, where it is joined to the base of the gantry. It needs to be affixed both to make a stable area for assembly, as many of the compliant techniques involve sliding, as well as to meet on-orbit requirements, where gravity will be low. For these experiments, the bottom (A) is attached with Velcro. The alignment for the bottom is done with an alignment jig, which the bottom's corner is pressed against. The compliance between the washer and the electromagnet allow the magnet to slide as the part itself is centered. After this, it is placed down, engaging the Velcro. This procedure is shown in Figure 4-2.

Figure 4-3: The procedure for installing the rails. First, it is brought to the assembly area, where it may be slightly askew (due to incomplete grip in the magnet, improper initial placement, or other anomalies). It is pressed to the hole in the base, which has chamfers around it to account for the error. It is then pressed in, allowing the chamfers to guide it to the correct position.

4.2.2 Place rail

Ideally, every item on the satellite would have an alignment jig similar to the bottom to help with assembly. However, because the satellite needs solar panels on the outside, it would require a complex external jig to align the adaptors.[1]. Instead, the rails are used not only to hold the solar panels in place, but to double as an alignment jig; because the rails are flush with the adaptors once installed, they can act as a corner to press into. The rail has compliance with the chamfers surrounding the hole it enters on the base. These chamfers were sized to account for the known precision of the robot; if the robot is commanded to place the rail into the center of the hole, even if it is off by the maximum amount of imprecision, the chamfers will guide it into place. For the non-southeast rails, the same procedure can be followed, with one additional benefit: the already-placed adaptors can act as alignment jigs for the rails, by pressing the inner corners together. This procedure is shown in Figure 4-3.

---

[1]This was considered. A jig could be designed such that the bottom base would slide underneath it, with an overhanging wall to press the adaptor against for alignment. A simple mock-up of this can be seen in Figure B-2 in Appendix B. After placing all adaptors, the whole satellite would be moved out to add the rails and the solar panels. This procedure was deemed to be too time intensive compared to simply using the rail.
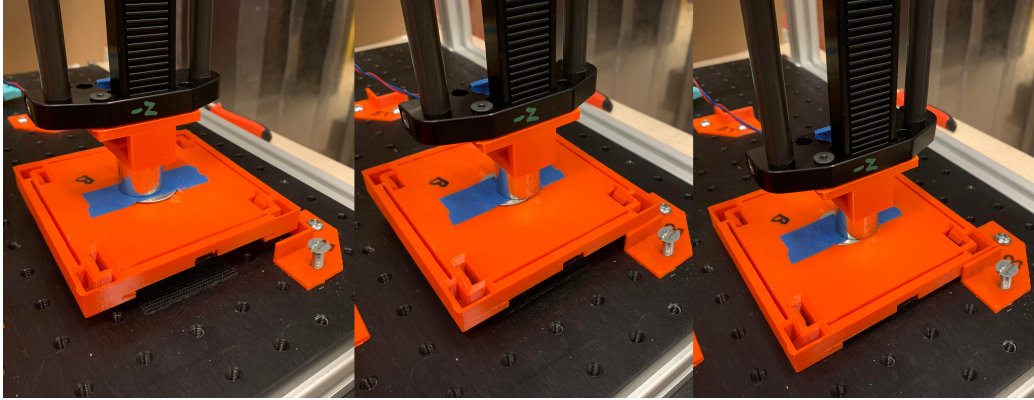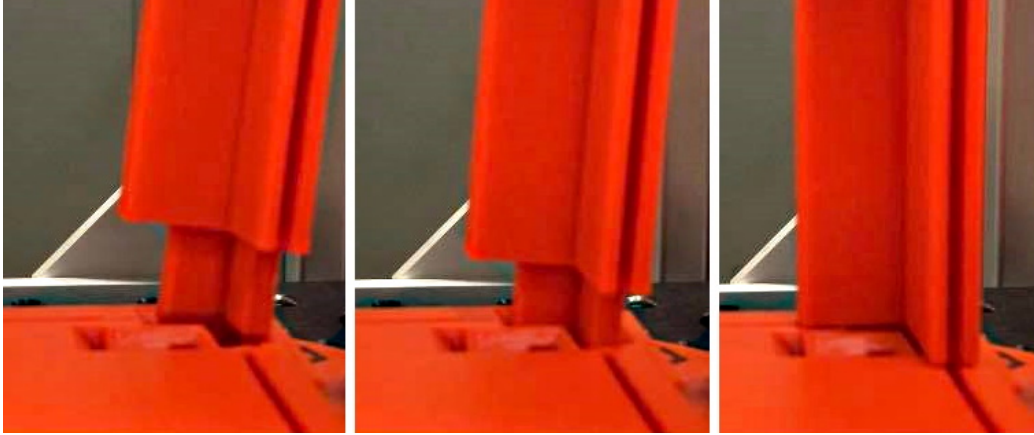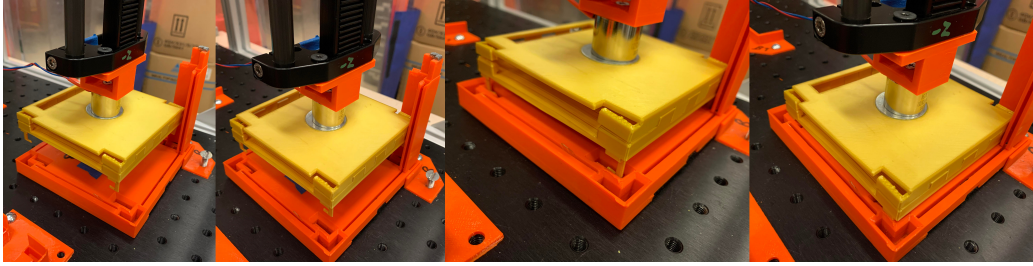
Figure 4-4: The procedure for installing an adaptor. First, it is brought to the assembly area, where it may be slightly askew (due to incomplete grip in the magnet, improper initial placement, or other anomalies). It is aligned using the rail. It is then pressed to just touching, after which the "wiggle" maneuver is performed. Then, it is pressed in.

4.2.3 Place adaptor

Each "place adaptor" procedure is the same. The adaptor is brought to the assembly area and pressed against the rail previously placed to line it up with the holes that are on the base or adaptor beneath. It is then lowered so it is just touching the surface of the part beneath it. A maneuver nicknamed "wiggle" is done to ensure the latches have been properly placed in their holes, by moving the adaptor slightly in four directions in the X-Y plane. The adaptor is then pressed in from the center, which should engage all four latches. To cover cases where a latch is not fully engaged, the gripper is then moved to press the adaptor in on the positive and negative Y sides by pressing down on the adaptor and sliding down the X axis. This is a secondary insertion method, and is often not required, but is designed to catch any anomalies. This procedure is shown in Figure 4-4, and the press-in step is shown in Figure 4-5.

4.2.4 Place solar panel

Although solar panel assembly is not done in this study, it was still considered. The solar panels would be gripped from the flat side to allow for a larger target area. Each rail has a chamfer at the top of it to allow the solar panel to slide into, where it is pressed into a slot in the base. Doing this should automatically engage the electronic

plug. It is possible an extra "wiggle" maneuver would be required to ensure it is aligned with the plug. In order to perform this, either the magnet needs to be able to be able to rotate to be in the X-Z or Y-Z planes, or the entire CubeSat would need to be rotated to slide the panels in sideways. Further discussion of this can be found in Chapter 6.

4.2.5 Place top

The top of the satellite presents an additional challenge, as it doesn't have any dedicated alignment jig to place it. Instead, it relies on the same methods used to insert the rails by centering the top and allowing the chamfers to cover any uncertainty in positioning when it is lowered into position. It is then pressed from the center, engaging the latches on its underside.

4.3 Performance Metrics

The primary method of assessing the success of the assembly is with qualitative analysis, whereby each trial was given a ranking of full success, partial success, or failure.

A **full success** is defined as a placement of a part with no faults, misalignments, or breakages. The part was placed properly the first time and fully inserted. There is no need for readjustment or modification. Examples of full success can be seen in the procedure diagrams (Figures 4-2, 4-4, and 4-3).

A **partial success** is defined as a placement of a part that was initially incorrect, but was corrected by the compliant design. Usually, this is seen as a latch that was not initially placed into its corresponding hole, but was able to be lined up up before it was inserted, either by a "wiggle" maneuver or the extra press-in step. Ultimately, the part was successfully placed. For the purposes of assessing the success of the

test procedure and the parts, a partial success is the most desirable outcome, as it indicates the compliant design features are successfully leading to assembly. One such partial success can be seen in Figure 4-5, where the adaptor would only go in with the extra press-in step that engages the chamfers.
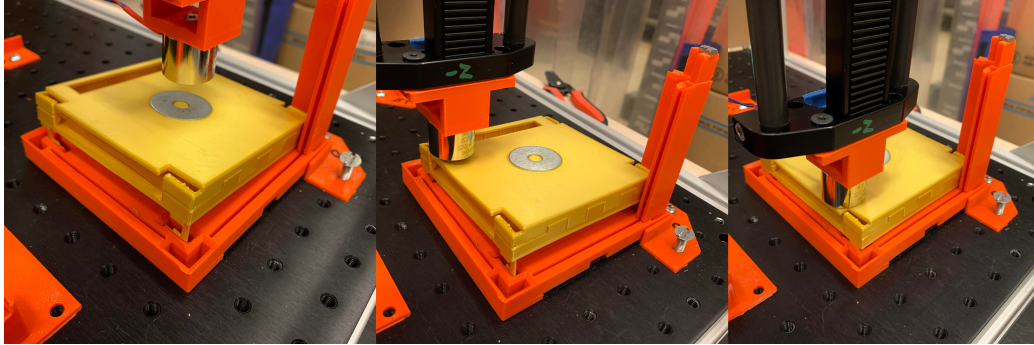
Figure 4-5: A partial success for an adaptor. After it is placed, it is askew (it could also be askew on the other side). Pressing it in on the sides engages the latches properly by having them slide along the chamfers.

A **failure** is defined as one of two things. The first is the placement of a part in which it does not reach the proper position by the time the robot moves on to the next step. It is very likely that, if assembly continues, the next part will not be able to be attached properly. Examples of this involve a rail missing the hole and still being attached to the end effector when it moves to the next part, an adaptor being knocked askew when it is placed, causing all the latches to miss the hole, and others.

The second type of failure is if a part is broken. This includes if a part is seemingly placed properly, but when it is taken apart to be examined, something had broken in the process. One example of this is if a latch was snapped after being pushed into place.

A statistical analysis is then performed on the performance to determine the significance level of the assembly. As was stated in the requirements in Chapter 2, we consider a part assembly that gets a significance level of 5%, or there being only a 5% chance the successes are random, as performing as planned. Each assembly was also timed, from the time the robot begins moving to the time it finishes moving.

Chapter 5

Results and Discussion

This chapter looks at the results of the robotic assembly tests, both qualitatively and with statistical analysis. First, it shows the results of each of the twenty trials for each part. Then, it discusses the performance of each of those parts in turn. Finally, is looks at some additional flaws and challenges that were encountered during and after the assembly tests.

5.1 Assembly Results

The results of the robotic CubeSat assembly tests are shown in Table 5.1. There are twenty trials for each part, and each is given a rating of success (green), partial success (yellow), or failure (red) (as described in Section 4.3). The average time given is the average of all successful and partially successful assembly times. Many of the failures did not result in assembly being completed. Additionally, all times are given with adjustments so that any times the robot was in an error state are removed (see Section 5.4). The full table of recorded times can be found in Table A.1 in Appendix A.

A one-tailed statistical hypothesis test is also performed to test the significance of finding this quantity of partial and/or complete successes. A hypothesis test finds if

Table 5.1: Qualitative assessment of assembly success, the average assembly time, and the statistical odds of getting the given results by random chance. Rails RNE, RNW, and RSW are the only statistically insignificant successes.

Part	Trial (1–20)	Avg Time [s]	Std Dev	p-value	H_o Status
Bottom (A)		9.96	0.09	9.5e-7	Reject
Rail RSE		9.413	0.39	0.0002	Reject
Adaptor B		17.239	0.70	0.0013	Reject
Adaptor C		27.662	1.52	0.0002	Reject
Adaptor D		30.965	1.84	0.0059	Reject
Adaptor E		32.98	2.42	0.0059	Reject
Adaptor F		27.665	0.72	0.002	Reject
Adaptor G		30.856	1.88	0.001	Reject
Rail RNE		9.582	0.50	0.588	Accept
Rail RNW		9.214	0.28	0.25	Accept
Rail RSW		9.332	0.18	0.942	Accept
Top (H)		12.3	0.50	9.5e-7	Reject

the demonstrated performance is statistically different from the "control" performance. In this case, we are looking to show that the successes and partial successes are occur often enough that it is more than 95% likely that it is not random chance if a part is successfully inserted. This defines the null hypothesis, H_o, as the success and failure being equally likely. If the calculated p-value (the probability of obtaining the observed results if successes were random) is less than 0.05, the null hypothesis is rejected, concluding it was not random whether it succeeded or not. The part design is effective. In Table 5.1, the calculated p-value and the status of H_o are shown.

5.2 Performance Analysis

5.2.1 Bottom

There was no problem accurately placing the base, with each trial being a full success. The alignment jig did its job each time, and the base was firmly placed into position. The only improvement that could be made is replacing the Velcro with a stronger method of attachment, as the base was still able to slide slightly during following assembly efforts. There is also the potential problem with Velcro that it could affix the base in the wrong spot if it was placed in the wrong position, as any surface area of Velcro touching connects it, although this was never seen during the trials.

5.2.2 Adaptors

All adaptors acted similarly, so they will be discussed in this section. The performance was generally mixed, but erred on needing the compliant design to insert properly; out of 120 adaptor trials, 59 were complete successes, 43 were partial successes, and 18 were failures.

Unlike the base, which had a sturdy alignment jig, the rail did not fit into the base snugly enough to ensure it could not move when the adaptor was pressed against it. The amount of deflection was minimal, but it often meant the latches were slightly off of the desired position for insertion, leading to a scenario for either a partial success or a failure. This was when the "wiggle" maneuver was key – the rail would get it close enough to correct such that the wiggle would catch the latches into the holes.

The extra press in step was required for all 43 partial successes as well, as the wiggle often did not have all four of the latches centered on the hole, and the first press in would only engage the two that were better placed. The extra press in step would then force the other two in by taking advantage of the chamfers.

The main source of the 18 complete failures was broken latches, with 14 of them being due to breakage. The breaking typically did not visibly occur while the structure was being assembled, but it was found when doing the post-assembly inspection. Sometimes, entire latches would have snapped off, and sometimes they would be partially broken off. This indicates that there is either more force being exerted on them than was expected, or the repeated insertion and removal weakened them (see Section 5.3). It is also possible that the compliant features currently used are insufficient to guarantee the latches are being directly inserted as intended. This corroborates with other complete failures, where the adaptor would be angled in such a way the "wiggle" maneuver could not get the latches aligned. The remaining 4 failures occurred due to the adaptor being placed far enough off the insertion location that the "wiggle" maneuver could not get it into place. This level of misalignment

was likely a combination of software problems (see Section 5.4), known imprecision in the motors, and RSE being pushed out of place.

5.2.3   Rails

In total, out of 80 rail trials, 45 were complete successes, 1 was a partial success, and 34 were failures. The rail being placed before the adaptors (RSE) performed much better than the three rails being placed after, with it being the only rail to have a statistically significant number of successes. This seems contradictory, as the assembly procedure is the same for both of them other than the adaptors already being in place. In theory, the adaptors should have only helped, as they provided a corner to rotate the rails into place. In practice, however, the problem came down to the strength of the magnet and the surface area of the lift point. The top of the rails were smaller than the magnetic gripper, so only a fraction of the grip force was being used. This amount was insufficient enough that, when the rail was lifted out of its starting area, it would occasionally rotate before settling. This slightly rotated rail was then brought to the adaptors. Intentionally, the rails were made to push up against the adaptors. However, because of the relatively weak grip strength, they were pushed askew instead of rotated, and would not insert properly. This accounted for all 32 of the collective failures for RNE, RNW, and RSW.

As seen from RSE, this issue was only present when the adaptors were obstacles for the rails; the small rotations when lifting initially were generally within the area of error that the chamfers on the base corrected for, and the 2 failures it experienced occurred when the rotation exceeded the chamfer correction area. The single partial success occurred for RSE when it landed slightly outside the chamfer area, but still managed to be pushed into the hole. All successes for RNE, RNW, and RSW were times when they did not come into contact with the adaptors, performing similarly to RSE.

5.2.4 Top

Despite having only the chamfers around the rails as a compliant design feature, as there was not an alignment jig for it, there were few issues with placing the top, with 19 successes and 1 partial success. Originally, a small wiggle maneuver was included in the top application procedure (similar to the adaptors, it would be brought down to touching, wiggle in all directions, then press in), but it was unnecessary, as it was properly aligned before the wiggle each time. The final tests were done without this maneuver, and only had one partial success, which occurred when the top was slightly askew, but the chamfers pushed it into place.

5.2.5 Full Assembly

There was no appreciable difference performing a full assembly than performing individual actions, other than timing problems (see Section 5.4).

5.3 Part Degradation

The structure was not designed to be put together and taken apart multiple times, as, once assembled on orbit, it will not be deconstructed. Because of this and the repeated use of the same parts rather than fabricating a lot of single-use parts, there was degradation in parts seen pre- and post- tests. The primary form of degradation was seen in the latches on the adaptors, and is shown in Figure 5-1. As expected, the cantilever experiences the most stress at its base. After multiple repeated assemblies, fractures appeared. The entire latch was angled off the vertical as well because of this, and was occasionally snapped off. If this was seen in-between trials, the adaptor was swapped out with one that was not broken, and the trial was marked as a failure. As discussed previously, this was the case for the majorities of the failures on adaptor tests (14/18). It is likely the continuous strain that lead to a fracture, and not the

individual test marked as a failure, as 9 of the 14 failures caused by breakages occurred at trial 13 or later.

A second form of degradation was found only after all tests were completed and the structure was deconstructed. Most adaptors had one or more of their latches sheared off, in particular, adaptors B and C had all four missing, and D and E had two missing. This was not observed after the twentieth assembly for those adaptors; after their twentieth assembly, as with all previous assembles, the adaptor was taken off, inspected, and then snapped back on by hand. The adaptor was not inspected again until all testing was completed. There are a few likely causes for the latch damage. There were a 4 incidents of adaptors colliding with the partially assembled structure or being pushed in when they were not in place. These could have put sideways loads on already installed adaptors with an unexpected amount of force. Another possible culprit is the "wiggle" maneuver. The lateral loads these applied to the structure were assumed to be minimal and thus were ignored, but they may have had more of an effect than anticipated. A final potential flaw could be in the disassembly procedure itself. To disassemble a board, the latch needs to be moved by hand to disengage with the outcropping below it. This force was also not designed for in the initial design and may have contributed to the degradation.

5.4   Robot Operation

The robot suffered from a few malfunctions that made it difficult to assess full reliability of the assembly procedure. As stated, all times in Table 5.1 are listed having subtracted the time the robot spent in an error state. A persistent error occurred where the robot would fail to move in the Z axis if it was the only axis in motion. This error was able to be self-corrected by re-sending the command, but it could lead to wait times of up to 30 seconds between individual movements of the robot in the
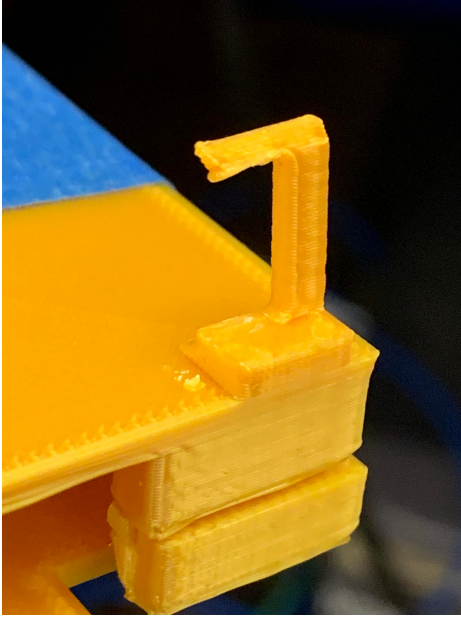
(a) A fracture on the base of a cantilever, as shown from the front.

(b) A fracture on the base of a cantilever, as shown from the back.

Figure 5-1: Degradation of the cantilever latches after 20 rounds of insertion testing. The cantilever is angled to the side, and there is a fracture at the base.

Z axis, which were required for lifting and placing the rails. This configuration issue made measuring accurate assembly times and even performing assembly difficult. The malfunction would need to be corrected in future work, either by replacing the node that was experiencing the error, or by modifying the motion planning to minimize the amount of time the Z axis is moved on its own.

5.5   Overall Assessment

The full assembly time averages to 3 minutes and 47 seconds, with an average standard deviation of approximately one second. All parts succeeded with the desired statistical significance, except RNE, RNW, and RSW. This shows that the assembly of all other parts is significant, and the procedure and design is successful. Additional damage to the latches was found after all tests were completed, so it is possible that there are unforeseen issues with assembly, and the cause of this needs to be isolated. However,

even if there are problems with the design, the results still suggest that only minor iterations will be necessary, rather than full redesigns.

Chapter 6

Conclusions and Future Work

6.1 Research Summary

This study assesses the capability of a low cost robot using minimal sensors to put together a custom 1U CubeSat structure. Requirements for the custom structure are created and a design to meet requirements is developed. The design leverages 3D printing techniques in order to utilize compliant design latches to allow a robot to snap the structure together without the need for screws or small fasteners. A STPA analysis is performed to ensure the safe procedure of both the testing and the on-orbit performance, and helps provide guidelines for safe programming, construction, and operation practices to be followed through each iteration of the system. The custom structure is put through assembly testing to determine its viability.

6.2 Contributions

This thesis has shown the feasibility for a Cartesian robot to assemble a 1U CubeSat. This assembly is done without any high end sensors, leveraging the robustness of compliant design. This demonstration shows that assembly can be done in approximately four minutes. This quick integration can support rapid deployment on-orbit.

This groundwork is crucial to constructing a functional 1U CubeSat, and eventually to constructing configurable nodes of multiple CubeSats on orbit. The demonstration has also revisited some requirements for initial part placement (for example, that consistency is key), which will aid in the design of the part delivery system.

6.3 Recommendations and Future Work

There are several areas needed to be expanded on to directly follow the work in this thesis, particularly in the structure design and the robot work.

6.3.1 Recommended Structure Adjustments

The best performing complaint design features were chamfers and alignment jigs, as the bottom (using alignment jigs), top (using chamfers), and the rail that was unimpeded (using chamfers) all had excellent assembly scores (100%, 90%, and 100% full or partial successes, respectively). Additional chamfers could likely be incorporated into the design of the holes on the adaptors to help improve their performance.

Using RSE as an alignment jig generally performed as intended, but its ability to be nudged out of position hindered its performance. These were the cases where the latches were misaligned, either needing to be corrected by the "wiggle" maneuver, as was seen in the 43 partial successes, or leading to one of 4 misalignment-caused total failures. There are several options that can help fix this. The friction between the rail and the bottom could be increased by making the hole in the bottom slightly smaller. Alternatively, the alignment jig used to place the bottom could be extended upwards, as seen in Figure 6-1. This would provide a harder stop to prevent deflections, but could potentially lead to the issue the other rails were encountering with collisions (see Section 6.3.2 for recommended fixes).

The cause of adaptor latches breaking should be isolated. The procedures for
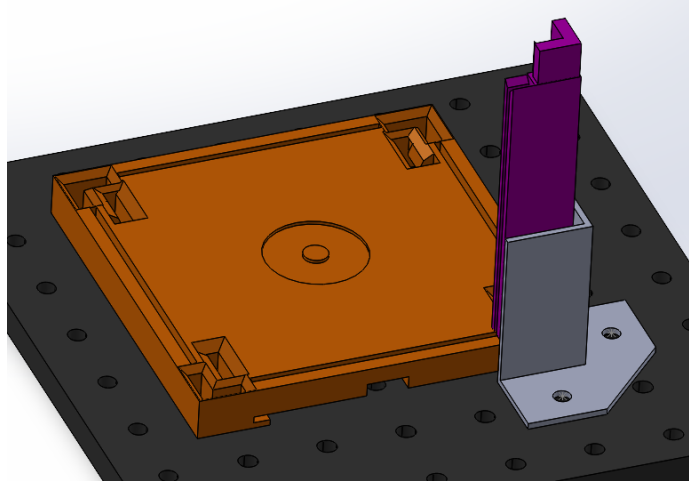
Figure 6-1: An extended version of the alignment jig for the base, providing support for the RSE. This would prevent RSE from deflecting, leading to alignment issues with the adaptors.

future assembly tested can be adjusted for this. Instead of performing assembly 20 times per part, assembly should be performed all at once with single-use boards to better simulate the designed-for performance. Additionally, the entire assembly should be examined after assembly is performed to verify there is no degradation. The "wiggle" maneuver should be simulated or otherwise quantified to determine if it is the cause of latches being broken. The maneuver can then be modified or removed as necessary. This will help isolate and mitigate the cause of rail degradation. If it is found that the plastic deflections are still leading to breakages, the latches could be redesigned to avoid this entirely. A small, spring-loaded system could be used that would allow the latch to deflect around the outcropping without putting strain on the latch itself. The cantilever latch could be on a small hinge with a spring connecting it to a non-deflecting wall. When the latch is pushed over an outcropping, it would compress the spring, moving the latch around the outcropping. When the latch reaches the opposite side of the outcropping, the spring would relax, straightening the rail and locking it in place. An early design of this can be seen in Figure 6-2. Although much more robust, this would require significantly more post-processing
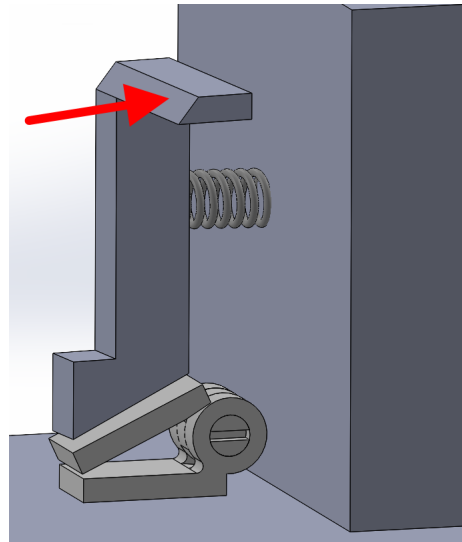
Figure 6-2: A sketch of a potential new version of the latch. When inserted, a force will be exerted on the latch where the red arrow is drawn. This will compress the spring and allow the latch to move around the outcropping. When it passes the outcropping and the force is no longer applied, the spring will relax and it will hold onto the outcropping.

work than simply 3D printing the latch. Manufacturing constraints would be analyzed in future work.

6.3.2   Recommended Robot Adjustments

The persistent error in the Z axis should be resolved, likely by replacing the controller, as it is suspected to be a hardware error. If it is not, changes could be made to the path planning algorithm to favor moving in the Z axis only in conjunction with moving in other axes, as this was seen to minimize the number of errors.

The gripper needs to have an additional degree of freedom added to it to allow for the installation of solar panels. A second electromagnet would need to be installed perpendicular to the first one to allow for lateral lifting of the panels. Then, this electromagnet would need to be able to rotate along the Z axis to allow the panels to be inserted on all four sides of the CubeSat. This capability could also be leveraged to help fix the issues with installing the rails, as they could also be lifted from the sides.

Lifting from the sides would increase the surface area of the magnetic attachment, and thus the connection would be strong. Another option to mitigate the rail assembly problem would be to replace the the gripper with a stronger electromagnet. The strength of this electromagnet may need to be variable by utilizing a simple dimmer to increase and decrease the current as necessary to allow for the compliant sliding when installing the bottom and the adaptors.

The main improvement, however, is to include more sensors to allow for full feedback control when performing assembly. This would allow for the assembly to be more robust, potentially preventing all assembly failures encountered in this study. There are three sensors being considered. First, the robot may need to be changed to be able to utilize limit switches to prevent localization problems. Second, a pressure sensor could be placed beneath the assembly area to check how much the robot is pressing down and be able to provide feedback to stop it if it exceeds a safe margin. This could be done by utilizing a piezoresistive, flat force sensor that changes its internal resistance when it is pressed upon. This reading could be integrated in the closed loop control. Another piece of control could be a camera that is providing direct feedback to the robot about the alignment of the parts before they are pressed together. To do this, the colors of each of the adaptors may need to be changed to allow for visual indications of alignment. Path planning algorithms should be analyzed for their use of re-planning when feedback is given to the system. These algorithms should be extended to situations where FOD may be introduced, such as if latches were to break, and simulations of this should be performed to ensure robust assembly. The autonomous system should be considered within a larger context of unauthorized remote access as well.

6.3.3 Recommended Next Steps

After making the adjustments discussed in Sections 6.3.1 and 6.3.2., the viability of pogo pins as electronic connectors should be assessed. Electronic boards with simple functions should be placed in the boards and assembled, and the required precision for connecting the pogo pins should be assessed. After this, functional CubeSat boards can be checked for compatibility with pogo pins. These boards would need to be modified to not only utilize pogo pins, but to not allow current to pass through them until assembly is completed. A system would need to be designed to verify the electrical connection between each board, and an external switch to powering the assembly would need to be added.

More ground stage demonstrations are necessary before the system can be moved to orbit. Mechanical testing must be repeated with the recommended changes to further improve the confidence with fully autonomous robotic assembly. Once the mechanical design is finalized, electronic testing can begin, first with pogo pins, then with functional CubeSat boards. The full system should undergo thermal-vacuum testing to verify the function of the robot, the custom structure, and the chosen CubeSat boards in vacuum environment. The system should additionally be tested in zero-gravity to verify that all assembly steps are compatible with it.

Appendix A

Tables

Table A.1: Time for each assembly trial, given in seconds. Red cells indicate the assembly was a failure and an accurate time could not be measured. Note that the table wraps, with tests 1-10 on the top and tests 11-20 on the bottom.

| Part	Trial									
	1	2	3	4	5	6	7	8	9	10
Bottom (A)	9.91	10.10	9.83	9.87	10.01	9.99	9.91	9.92	10.01	9.88
Rail RSE	9.41	9.50	10.37	9.98		10.14	9.63	9.13	9.04	9.39
Adaptor B	17.41	17.33	17.65	14.86	17.40	17.20			17.30	17.76
Adaptor C	27.09	26.89	26.90	27.60	27.70	26.09	30.88	31.27	30.35	26.74
Adaptor D		30.82	26.71	32.80	31.29	32.79	28.47	31.71	32.77	30.28
Adaptor E		32.20	33.76		30.01	30.22	31.00	30.28	34.25	36.50
Adaptor F	27.64	26.92	27.56	28.25	28.20	26.11	27.21	26.93		27.12
Adaptor G	30.82	33.10	32.10	33.51	28.88	29.10	32.12	28.24	29.25	30.52
Rail RNE				9.90	8.94	9.82	9.93	10.01		
Rail RNW	9.85	9.54	9.10	9.54		9.08	8.89			
Rail RSW			9.28					9.39		
Top (H)	12.00	11.45	12.88	12.87	12.52	11.87	12.57	11.11	11.56	12.15
	11	12	13	14	15	16	17	18	19	20
Bottom (A)	10.04	9.93	9.88	10.20	9.87	9.94	10.01	9.99	9.89	10.00
Rail RSE	9.16	9.41	9.20	9.23	9.20	9.17		9.47	9.01	9.01
Adaptor B	17.50	17.36		17.48	17.26	18.11		17.16	17.32	17.75
Adaptor C	26.57	27.41		26.79	27.46	26.97	27.03		27.06	27.09
Adaptor D	29.36	33.62	29.01	31.10	29.95		30.02	31.11	32.53	33.03
Adaptor E	32.22	33.87	32.86	36.62	36.66	30.33	31.31			35.56
Adaptor F	26.85	28.55	29.10	28.12		27.52	28.10	27.78	28.10	27.99
Adaptor G	29.20	33.20	33.51	30.12	29.10		30.60	33.20		28.83
Rail RNE			8.80		9.93			9.04	9.88	
Rail RNW	9.01	9.15	9.08	9.15	9.25				8.95	
Rail RSW		9.42		9.25	9.01	9.58				9.42
Top (H)	12.74	12.56	12.10	12.55	12.35	12.65	12.78	12.19	12.88	12.41

Appendix B

Figures
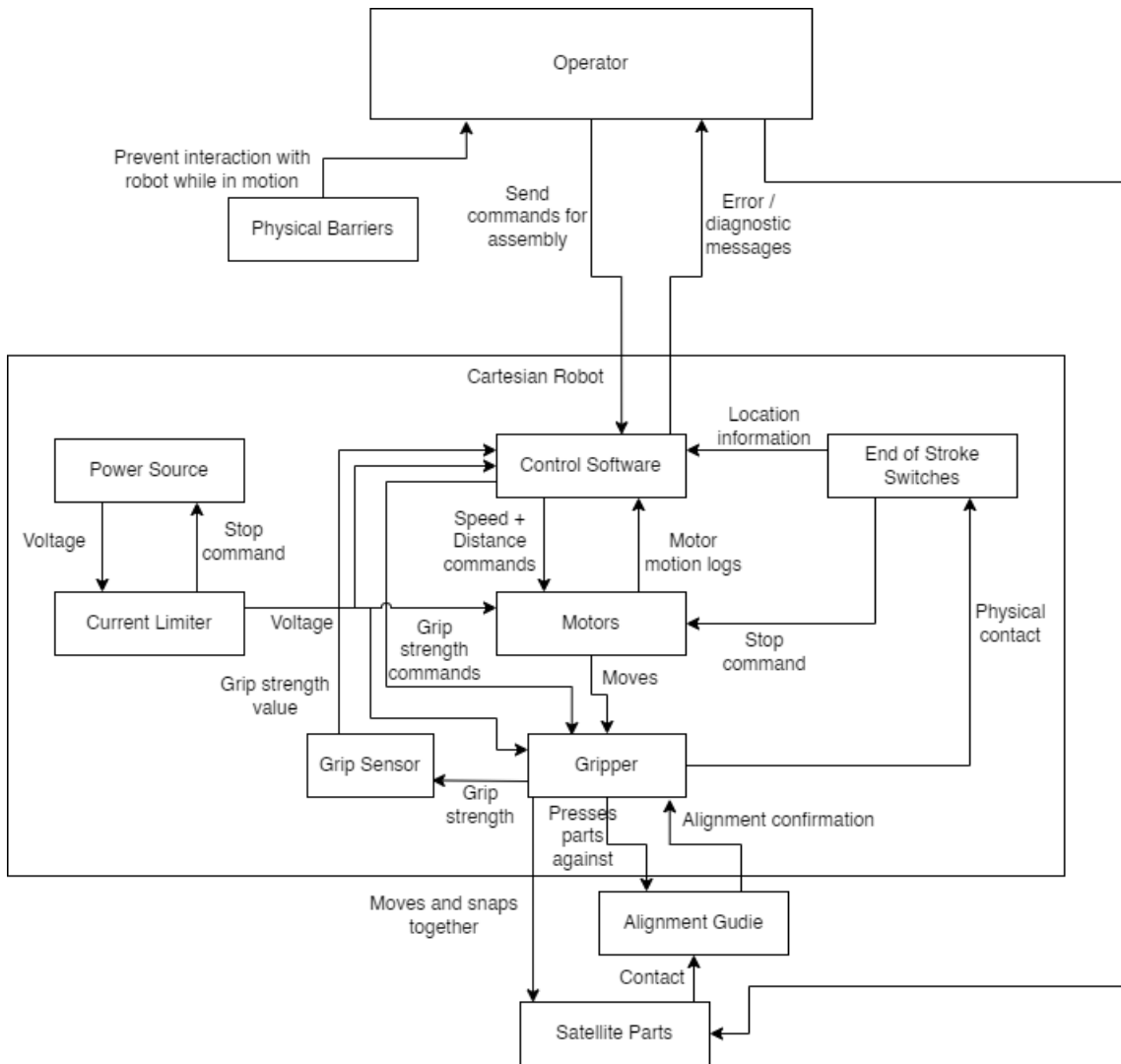
Figure B-1: A refined version of the robot control structure on the test bed. This version is for the finger gripper.
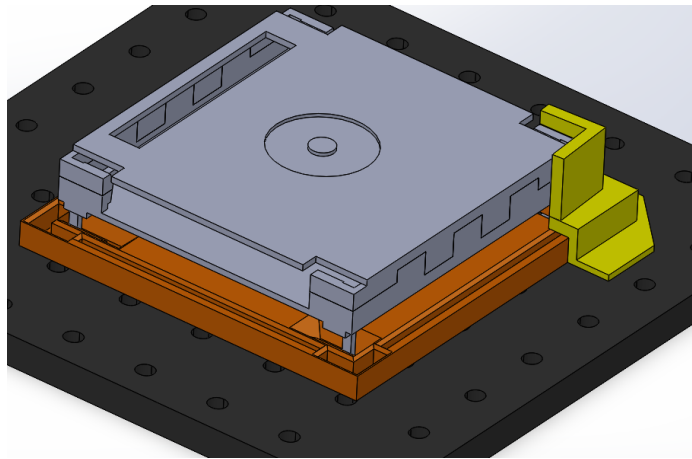
Figure B-2: The proposed alignment jig for the adaptors. It would require sliding the bottom underneath it, and thus would require the whole satellite to be moved in order to install the rails and solar panels.

This page is intentionally blank.

Bibliography

[1] European Space Agency (ESA). *Outgassing Database*. URL: http://esmat.esa.int/services/outgassing_data/outgassing_data.html (visited on 04/01/2022).

[2] *3D Printed Satellite Exterior | NASA Case Study | Stratasys Direct*. URL: https://www.stratasysdirect.com/resources/case-studies/3d-printed-satellite-exterior-nasa-jet-propulsion-laboratory (visited on 04/01/2022).

[3] National Aeronautics and Space Administration. *Outgassing Data for Advanced Search and Report*. URL: https://outgassing.nasa.gov/cgi/uncgi/search/search_html_ad.sh. (visited on 04/01/2022).

[4] Q A Bean et al. "INTERNATIONAL SPACE STATION (ISS) 3D PRINTER PERFORMANCE AND MATERIAL CHARACTERIZATION METHODOLOGY". en. In: (June 2015), p. 11.

[5] Iain D. Boyd et al. *On-Orbit Manufacturing and Assembly of Spacecraft*. Jan. 2017.

[6] Chantal Cappelletti. "Structure, new materials, and new manufacturing technologies". en. In: *Cubesat Handbook*. Elsevier, 2021, pp. 165–183. ISBN: 978-0-12-817884-3. DOI: 10.1016/B978-0-12-817884-3.00008-4. URL: https://linkinghub.elsevier.com/retrieve/pii/B9780128178843000084 (visited on 04/01/2022).

[7] Joseph Carsten, Dave Ferguson, and Anthony Stentz. "3D Field D: Improved Path Planning and Replanning in Three Dimensions". In: *2006 IEEE/RSJ International Conference on Intelligent Robots and Systems*. ISSN: 2153-0866. Oct. 2006, pp. 3381–3386. DOI: 10.1109/IROS.2006.282516.

[8] T Clements et al. "3D Printed Parts for Cubesats; Experiences from Kysat-2 and Printsat Using Windform XT 2.0". In: *Proc. 2nd Int. Acad. Astronaut. Conf. Dyn. Control Sp. Syst.* 2015.

[9] *CONFERS*. en-US. URL: https://www.satelliteconfers.org/ (visited on 04/26/2022).

[10] *CubeSat Design Specification Rev. 12*. 2012.

[11] Daria Derusova et al. "Nondestructive Testing of CubSat Satellite Body Using Laser Vibrometry". In: *Russian Journal of Nondestructive Testing* 55 (May 2019), pp. 418–425. DOI: 10.1134/S1061830919050024.

[12] Samuel Hunt Drake. "Using compliance in lieu of sensory feed- back for automatic assembly". Ph.D. dissertation. Massachusetts Institute of Technology, 1977.

[13] Daniel Fluitt. "Feasibility Study Into the Use of 3D Printed Materials in CubeSat Flight Missions". en. PhD thesis. San Luis Obispo, California: California Polytechnic State University, June 2012. DOI: 10.15368/theses.2012.122. URL: http://digitalcommons.calpoly.edu/theses/805 (visited on 04/01/2022).

[14] John Gregory et al. "Characterization of Semi-Autonomous On-Orbit Assembly CubeSat Constellation". In: *Small Satellite Conference* (Aug. 2019). URL: https://digitalcommons.usu.edu/smallsat/2019/all2019/30.

[15] Braden Grim et al. *MakerSat: A CubeSat Designed for In-Space Assembly*. Aug. 2016.

[16] Ansley N Knight et al. "Design and Development of On-orbit Servicing CubeSat-class Satellite". en. In: *SmallSat 2020* (July 2020), p. 10.

[17] Sven Koenig and Maxim Likhachev. "D*Lite." In: *Proceedings of the National Conference on Artificial Intelligence*. Jan. 2002, pp. 476–483.

[18] Erik Kulu. *Nanosatellites Through 2020 and Beyond*. Apr. 2021. URL: http://mstl.atl.calpoly.edu/~workshop/archive/2021/presentations/Day%201/Trends,%20Databases%20&%20Standards/Erik%20Kulu.pdf.

[19] Nancy G. Leveson. *Engineering a Safer World: Systems Thinking Applied to Safety*. The MIT Press, Jan. 2012. ISBN: 978-0-262-29824-7. DOI: 10.7551/mitpress/8179.001.0001. URL: https://doi.org/10.7551/mitpress/8179.001.0001 (visited on 03/30/2022).

[20] Morgan McFall-Johnsen. *About 1 in 40 of SpaceX's Starlink satellites may have failed. That's not too bad, but across a 42,000-spacecraft constellation it could spark a crisis*. en-US. Nov. 2020. URL: https://www.businessinsider.com/spacex-starlink-internet-satellites-percent-failure-rate-space-debris-risk-2020-10 (visited on 04/26/2022).

[21] *Momentus Space: Services*. en-US. URL: https://momentus.space/services/ (visited on 05/10/2022).

[22] Gilbert Moore et al. "3D Printing and MEMS Propulsion for the RAMPART 2U CUBESAT". In: 2010.

[23] Giorgio Musso et al. "Portable on Orbit Printer 3D: 1st European Additive Manufacturing Machine on International Space Station". In: vol. 489. Jan. 2016, pp. 643–655. ISBN: 978-3-319-41693-9. DOI: 10.1007/978-3-319-41694-6_62.

[24] E.J. Nicolson and R.S. Fearing. "Compliant control of threaded fastener insertion". In: *[1993] Proceedings IEEE International Conference on Robotics and Automation*. May 1993, 484–490 vol.1. DOI: 10.1109/ROBOT.1993.292026.

[25] Ted Nye, Andrew Schurr, and Mark Milam. "Development of a MicroSat for On-Orbit Satellite Surgery". en. In: (Aug. 2019), p. 11.

[26] Simon Patane et al. "Archinaut: In-Space Manufacturing and Assembly for Next-Generation Space Habitats". en. In: *AIAA SPACE and Astronautics Forum and Exposition*. Orlando, FL: American Institute of Aeronautics and Astronautics, Sept. 2017. ISBN: 978-1-62410-483-1. DOI: `10.2514/6.2017-5227`. URL: `https://arc.aiaa.org/doi/10.2514/6.2017-5227` (visited on 04/26/2022).

[27] *Phoenix*. URL: `https://www.darpa.mil/program/phoenix` (visited on 04/26/2022).

[28] Jacopo Piattoni et al. "Plastic Cubesat: An innovative and low-cost way to perform applied space research and hands-on education". en. In: *Acta Astronautica* 81.2 (Dec. 2012), pp. 419–429. ISSN: 00945765. DOI: `10.1016/j.actaastro.2012.07.030`. URL: `https://linkinghub.elsevier.com/retrieve/pii/S0094576512002937` (visited on 04/25/2022).

[29] S. Pitipong, P. Pornjit, and P. Watcharin. "An automated four-DOF robot screw fastening using visual servo". In: *2010 IEEE/SICE International Symposium on System Integration*. Dec. 2010, pp. 379–383. DOI: `10.1109/SII.2010.5708355`.

[30] *PrintSat*. en. URL: `https://space.skyrocket.de/doc_sdat/printsat.htm` (visited on 04/27/2022).

[31] *Robotic Servicing of Geosynchronous Satellites*. URL: `https://www.darpa.mil/program/robotic-servicing-of-geosynchronous-satellites` (visited on 04/26/2022).

[32] Corey Shemelya et al. "Multi-functional 3D printed and embedded sensors for satellite qualification structures". In: *2015 IEEE SENSORS*. Nov. 2015, pp. 1–4. DOI: `10.1109/ICSENS.2015.7370541`.

[33] *Stratasys: ULTEM 9085 Datasheet*. URL: `https://www.stratasys.com/-/media/files/material-spec-sheets/mss_fdm_ultem9085_1117a.pdf` (visited on 04/11/2022).

[34] Ezinne Uzo-Okoro. "Characterization of on-orbit robotic assembly". S.M. Massachusetts Institute of Technology, 2020.

[35] Ezinne Uzo-Okoro et al. "Ground-Based 1U CubeSat Robotic Assembly Demonstration". In: *Small Satellite Conference* (Aug. 2020). URL: `https://digitalcommons.usu.edu/smallsat/2020/all2020/5`.

[36] Ezinne Uzo-Okoro et al. "Optimization of On-Orbit Robotic Assembly of Small Satellites". In: *ASCEND 2020*. _eprint: https://arc.aiaa.org/doi/pdf/10.2514/6.2020-4195. American Institute of Aeronautics and Astronautics, Nov. 2020. DOI: `10.2514/6.2020-4195`. URL: `https://arc.aiaa.org/doi/abs/10.2514/6.2020-4195` (visited on 04/25/2022).

[37] Thyrso Villela et al. "Towards the Thousandth CubeSat: A Statistical Overview". en. In: *International Journal of Aerospace Engineering* 2019 (Jan. 2019), pp. 1–13. ISSN: 1687-5966, 1687-5974. DOI: `10.1155/2019/5063145`. URL: `https://www.hindawi.com/journals/ijae/2019/5063145/` (visited on 04/22/2022).

[38] Mary J. Werkheiser et al. "3D Printing In Zero-G ISS Technology Demonstration". en. In: *AIAA SPACE 2014 Conference and Exposition*. San Diego, CA: American Institute of Aeronautics and Astronautics, Aug. 2014. ISBN: 978-1-62410-257-8. DOI: `10.2514/6.2014-4470`. URL: `https://arc.aiaa.org/doi/10.2514/6.2014-4470` (visited on 04/01/2022).

[39] *Windform XT 2.0 Datasheet*. URL: `https://www.windform.com/PDF/SCHEDA_WF_XT_2_0_ENG.pdf` (visited on 04/11/2022).

[40] William Yerazunis, Avishai Weiss, and Patryk P. Radyjowski. "On-Orbit Additive Manufacturing of Parabolic Reflector via Solar Photopolymerization". In: International Astronautical Congress (IAC), 2019.